






# Spatial resolution impacts projected plant responses to climate change on topographically complex islands

Jairo Patiño<sup>1,2</sup>  | Flavien Collart<sup>3</sup>  | Alain Vanderpoorten<sup>4</sup> | José Luis Martin-Esquivel<sup>5</sup>  | Agustín Naranjo-Cigala<sup>6</sup>  | Sébastien Mirolo<sup>2,4</sup> | Dirk N. Karger<sup>7</sup> 

<sup>1</sup>Island Ecology and Evolution Research Group, Instituto de Productos Naturales y Agrobiología, Consejo Superior de Investigaciones Científicas (IPNA-CSIC), Tenerife, Spain

<sup>2</sup>Department of Botany, Ecology and Plant Physiology, University of La Laguna, Tenerife, Spain

<sup>3</sup>Department of Ecology and Evolution (DEE), University of Lausanne, Lausanne, Switzerland

<sup>4</sup>Institute of Botany, University of Liège, Liège, Belgium

<sup>5</sup>Teide National Park, Tenerife, Spain

<sup>6</sup>Departamento de Geografía, Universidad de Las Palmas de Gran Canaria, Las Palmas de Gran Canaria, Spain

<sup>7</sup>Swiss Federal Research Institute WSL, Birmensdorf, Switzerland

## Correspondence

Jairo Patiño, Island Ecology and Evolution Research Group, Instituto de Productos Naturales y Agrobiología, Consejo Superior de Investigaciones Científicas (IPNA-CSIC), Tenerife, Canary Islands, Spain.

Email: [jpatino@ipna.csic.es](mailto:jpatino@ipna.csic.es)

Flavien Collart, Department of Ecology and Evolution (DEE), University of Lausanne, Lausanne, Switzerland.

Email: [flavien.collart@unil.ch](mailto:flavien.collart@unil.ch)

## Funding information

Fundación BBVA, Grant/Award Number: PR19\_ECO\_0046; Ministerio de Ciencia e Innovación, Grant/Award Number: PID2019-110538GA-I00 and RYC-2016-20506; Ministerio para la Transición

## Abstract

**Aim:** Understanding how grain size affects our ability to characterize species responses to ongoing climate change is of crucial importance in the context of an increasing awareness for the substantial difference that exists between coarse spatial resolution macroclimatic data sets and the microclimate actually experienced by organisms. Climate change impacts on biodiversity are expected to peak in mountain areas, wherein the differences between macro and microclimates are precisely the largest. Based on a newly generated fine-scale environmental data for the Canary Islands, we assessed whether data at 100 m resolution is able to provide more accurate predictions than available data at 1 km resolution. We also analysed how future climate suitability predictions of island endemic bryophytes differ depending on the grain size of grids.

**Location:** Canary Islands.

**Time period:** Present (1979–2013) and late-century (2071–2100).

**Taxa:** Bryophytes.

**Methods:** We compared the accuracy and spatial predictions using ensemble of small models for 14 Macaronesian endemic bryophyte species. We used two climate data sets: CHELSA v1.2 (~1 km) and CanaryClim v1.0 (100 m), a downscaled version of the latter utilizing data from local weather stations. CanaryClim also encompasses future climate data from five individual model intercomparison projects for three warming shared socio-economic pathways.

**Results:** Species distribution models generated from CHELSA and CanaryClim exhibited a similar accuracy, but CanaryClim predicted buffered warming trends in mid-elevation ridges. CanaryClim consistently returned higher proportions of newly suitable pixels (8%–28%) than CHELSA models (0%–3%). Consequently, the proportion of species predicted to occupy pixels of uncertain suitability was higher with CHELSA (3–8 species) than with CanaryClim (0–2 species).

Jairo Patiño and Flavien Collart have contributed equally to this work.

This is an open access article under the terms of the [Creative Commons Attribution](https://creativecommons.org/licenses/by/4.0/) License, which permits use, distribution and reproduction in any medium, provided the original work is properly cited.

© 2023 The Authors. *Diversity and Distributions* published by John Wiley & Sons Ltd.

Ecológica y el Reto Demográfico,  
Grant/Award Number: 2941/2022;  
Schweizerischer Nationalfonds zur  
Förderung der Wissenschaftlichen  
Forschung, Grant/Award Number: 197777

Editor: Boris Leroy

**Main conclusions:** The resolution of climate data impacted the predictions rather than the performance of species distribution models. Our results highlight the crucial role that fine-resolution climate data sets can play in predicting the potential distribution of both microrefugia and new suitable range under warming climate.

**KEYWORDS**

bryophytes, Canary Islands, climate warming, microrefugia, range shift, species distribution models

## 1 | INTRODUCTION

Earth system models have played a crucial role for documenting climatic conditions at large spatial scales and predicting the consequences of past and future climate change (Moss et al., 2010; Thuiller et al., 2019). The availability of such data anywhere has boosted biological, ecological and conservation research over the past decades (Pereira et al., 2010). However, earth system models often smooth topographical and other associated environmental gradients (Rummukainen, 2010; Tapiador et al., 2020). The coarse spatial resolution of the resulting climatic data has increasingly raised concerns regarding the mismatch between the microclimatic conditions that organisms actually experience in the wild and the macroclimate (Rummukainen, 2010). In fact, macroclimatic conditions are often downscaled at 1 km<sup>2</sup> or more from coarser grids (25–100 km; Karger et al., 2017), thereby failing to capture the spatiotemporal variability in microclimate driven by, for instance, terrain, wind and vegetation (Maclean, 2020). Differences between macro- and microclimate are expected to increase in response to increasing differences in local elevation and topographic complexity. In particular, mountain rugged regions are expected to exhibit very decoupled macro- and microclimatic conditions, where microclimate can vary noticeably over very short distances (Dobrowski, 2011; Dobrowski et al., 2009; Graae et al., 2018; Lembrechts, Nijs & Lenoir, 2019). Spatial variability in microclimate greatly exceeds the magnitude of climate change expected in the upcoming century. Ignoring this variation has led to conflicting predictions of climate change impacts on species distributions (Maclean, 2020; Moudrý et al., 2023).

Regional climate models provide a complementary approach to generate fine-scaled climate data from tens to a few hundreds of meters (Giorgi, 2019). In practice, regional climate models are produced by dynamically downscaling earth system model outputs (e.g. by using the latter as boundary conditions and resolving local climate processes at a higher spatial resolution). An increasing number of studies have compared the accuracy and performance of species distribution models depending on the spatial resolution of the climate data (e.g., Ashcroft et al., 2012; Chauvier et al., 2022; Finocchiaro et al., 2023; Lenoir et al., 2017; Potter et al., 2013). Even if the idea that finer scale models lead to an improvement of model accuracy has not been consistently supported (e.g. Connor et al., 2018; Guisan et al., 2007; Manzoor et al., 2018; Moudrý et al., 2023; Stark & Fridley, 2022), the need for fine-scale climate

data becomes evident in mountain areas, where climate can vary at short scales of 10–100 m. In such rugged areas, topographic variation locally brings about suitable conditions for the existence of small, sheltered areas against climate change. These areas, whose local conditions are to some extent decoupled from the prevailing macroclimate (Dobrowski, 2011), can play an important role as microrefugia, namely for warm- and drought-sensitive organisms in a warming world (Finocchiaro et al., 2023; Hylander et al., 2015; Suggitt et al., 2018).

The availability of fine-scale climatic data, in order to identify putative microrefugia under global climate change, is particularly relevant in oceanic islands (Harter et al., 2015). These insular systems typically represent biodiversity hotspots for hosting large arrays of species characterized by both high rates of endemism and small population sizes and, hence, potentially high threat levels (Whittaker & Fernández-Palacios, 2007). While fine-scale microclimatic data were generated for the oceanic archipelagos of the Azores and Madeira (Azevedo et al., 1999; Santos et al., 2004) and Hawai'i (Berio Fortini et al., 2022), this is not the case for a number of other key archipelagos, such as the Canary Islands. Moreover, comparative studies of climatic models at different spatial resolutions remain virtually inexistent in the island literature.

The wide elevational, size, and climate variations among the islands of the Canarian archipelago shape the diversity of habitats they host, ranging from desert and semi-arid vegetation to montane cloud (humid) laurel forests and alpine scrublands. In the montane cloud forest, for example, the topographic transition from ravines to montane ridges is associated with strong turnover rates of plant communities across distances less than 500 m (del Arco-Aguilar et al., 2010; del Arco-Aguilar & Rodríguez-Delgado, 2018). The wide range of environmental conditions, coupled with geographic isolation among islands and between islands and continents, have triggered the evolution of high levels of endemism. Specifically, no less than 94% of terrestrial mollusc, all reptile, and almost 50% of native spermatophyte species are endemic to the Canary Islands (for a review see Florencio et al., 2021). The Canary Islands are therefore part of one of the world's 25 recognized biodiversity hotspots, and one of the most relevant floristic regions within the Mediterranean-type climate regions (Brooks et al., 2006; Mittermeier et al., 2005).

The unique terrestrial biodiversity of the Canary Islands is, however, under considerable threat due to habitat loss, biological

invasions and climate change. The Canary Islands are in fact within a climate change hotspot that has been projected to be highly impacted by climate warming and associated changing disturbance–climate interactions (Cos et al., 2021; Giorgi & Lionello, 2008). These climate change impacts have been suggested to be more pervasive in both alpine habitats and mid-elevation ridges (Martín et al., 2012; Patiño et al., 2016). Despite the long-standing interest in Canarian biodiversity (Florencio et al., 2021), our knowledge of the fine-scale climatic conditions species experience, how these conditions varied in the past, and whether they are likely to vary in the future, is still very limited. Such a limitation jeopardizes our ability to establish a clear link between species distributions and climatic conditions, and forecast their future ranges under changing climatic conditions. To bridge this gap, we present CanaryClim, a new climatic model at 100-m resolution for the Canary Islands. As a case study, we revisited previous assessments of climate change impacts on the Macaronesian endemic bryophyte flora in the Canary Islands based on 1-km resolution climatic data (Patiño et al., 2016), using the newly generated CanaryClim layers under three contrasted shared socio-economic pathways of warming climate (O'Neill et al., 2016).

Bryophytes are spore-producing land plants, whose distinctive ecophysiological traits make them ideal candidates for exploring the impact of climate change (Patiño et al., 2022). First, bryophytes are poikilohydric, which means that their water content is directly regulated by environmental humidity and precipitation. During periods of desiccation, bryophytes enter dormancy and stop physiological activity. Bryophyte species, however, exhibit important differences in the degree of desiccation they can tolerate. For instance, certain cloud forest species often exhibit anatomical adaptations for water storage. Such traits have been, however, proved to be suitable for coping with short-term drought resistance rather than long-term desiccation tolerance (reviewed in Proctor et al., 2007). Second, while they cope well with low-temperature regimes, bryophytes are more sensitive to moderately high temperatures. As an example,

a selection of boreal and temperate species die after a few weeks if temperatures are maintained above ca. 30°C (reviewed in He et al., 2016). Therefore, bryophytes typically occur in microhabitats with specific local climatic conditions, making them able to survive in areas where higher plants vanished due to climate change (He et al., 2016; Tuba et al., 2011).

In this context, the primary goal of this study was to assess the predictive performance of two climate data sets with different spatial grains (*sensu* Moudrý et al., 2023). This task was performed under warmed climate scenarios, including the macroclimate model from CHELSA v2.1 at 30-arc-second resolution (~1 km) and the newly downscaled climate grids from CanaryClim v1.0 at 100-m resolution. Based on these two climate data sets, we also analyse spatial and temporal differences in predicted climate suitability depending on grid size. Specifically, we tackle the following questions by comparing the CanaryClim and CHELSA data sets: Is there a difference of accuracy among species distribution models (SDMs) depending on the resolution of the climatic data? How do the projections of these models vary spatially under present and future conditions? To what extent does the newly generated, higher resolution CanaryClim data set allow for the identification of climate change microrefugia (*sensu* Bennett & Provan, 2008; De Frenne et al., 2021; Rull, 2009), or for the prediction of new climatic habitat range?

## 2 | METHODS

### 2.1 | Study area and species occurrence data

The study area covered the oceanic archipelago of the Canary Islands with a total area of 7492 km<sup>2</sup>, eight main islands and a number of islets (Figure 1). The archipelago is characterized by a general subtropical Mediterranean climate with strong gradients in temperature and precipitation depending on elevation, topography and longitude (del Arco-Aguilar et al., 2010; del Arco-Aguilar &

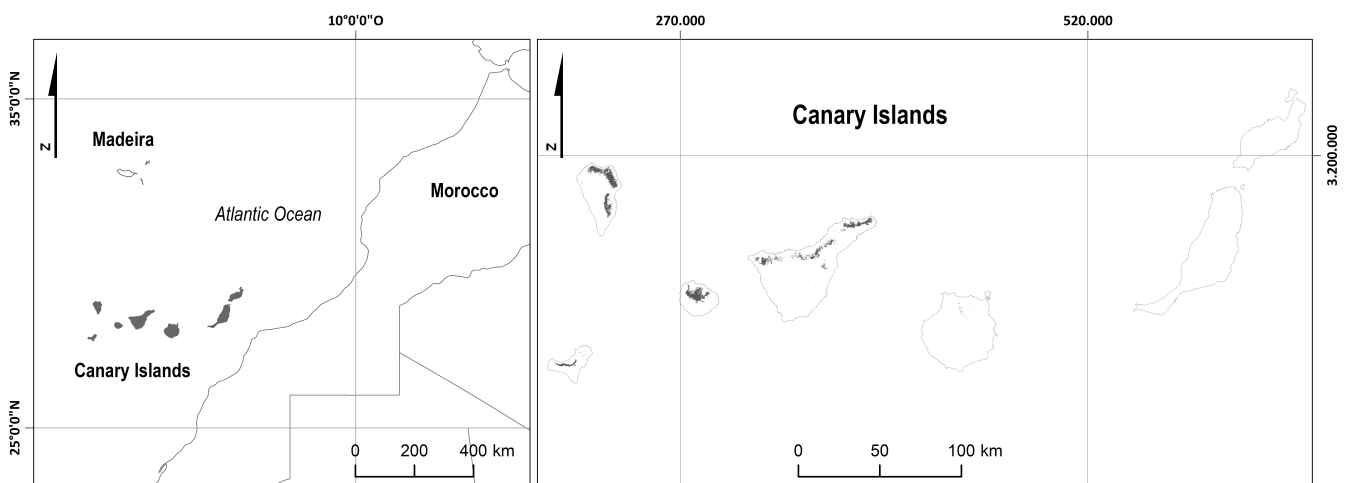


**FIGURE 1** Study area and current distribution of the montane cloud laurel forest, one of the main zonal ecosystems in the archipelago of the Canary Islands.

Rodríguez-Delgado, 2018). Thus, while the western and central islands are characterized by high, complex topographies and relatively humid climates, the eastern ones are flatter, topographically simpler and drier. Such differences explain the broader array of zonal ecosystems found on the highest islands compared with the lowest ones, wherein the first ones include from arid and semi-arid coastal scrubs, through semi-arid thermophilous woodlands, montane cloud laurel forests and xeric pine forests to summit alpine scrubs (del Arco-Aguilar et al., 2010; del Arco-Aguilar & Rodríguez-Delgado, 2018). The lower, eastern islands only preserve a representation of arid and semi-arid coastal scrubs.

To test the performance of species distribution models at contrasted spatial resolutions, we considered the 19 Macaronesian endemic bryophyte species present in the Canary Islands, except *Rhynchostegiella macilenta* which is now considered to be conspecific with *R. tenerifae* (Patiño, Hedenäs et al., 2017). The endemic element of the Canarian bryophyte flora is largely restricted (ca. 87%) to the montane cloud laurel forest (Patiño et al., 2014; Vanderpoorten et al., 2011). Species distributions were obtained from Patiño et al. (2016). This database was updated and additionally complemented for this work with recent verified herbarium records, thorough literature reviews and field observations (Figure S1 and Table S1). In total, 697 occurrences were obtained for 17 endemic bryophyte species. To avoid geographical sampling bias (sensu Syfert et al., 2013), we only retained occurrences that were separated by at least 100m from each other, matching the resolution of the CanaryClim data. Species occurring in <100m grid cells were removed (Jiménez-Valverde, 2020), including *Orthotrichum handiense* and *Aloina humilis*. We thus ended up with 14 Macaronesian endemic species, namely: *Cololejeunea schaeferi*, *Exsertotheca intermedia*, *Fissidens coacervatus*, *Frullania polysticta*, *Grimmia curviseta*, *Homalothecium mandonii*, *Leptodon longisetus*, *Leucodon canariensis*, *L. treleasei*, *Pelekium atlanticum*, *Plagiochila maderensis*, *Rhynchostegiella bourgaeana*, *R. pseudolitorea* and *R. trichophylla*. Nomenclature (Table S1) follows Hodgetts et al. (2020). The final species data set comprised 10–100 occurrences (with a median of 26.5), which was kept constant through the two resolutions allowing that the exact same number of occurrences is used for CHELSA SDMs. Although occurrence repetition can impact SDMs at 1 km (Varela et al., 2014), the number of duplicate occurrences in a pixel of 1 km was only, in median, two for nine out of 14 species. This represents approximately 7% of the total data set, suggesting limited autocorrelation.

## 2.2 | Climate variables

In order to generate the CanaryClim v1.0 climate data set, we down-scaled the global climate model of CHELSA v1.2 (Karger et al., 2017) and generated an ensemble of high-resolution climate data within the Sixth Assessment Report of the Intergovernmental Panel on Climate Change (CMIP6). The methodology applied is explained in the following sections.

### 2.2.1 | Precipitation downscaling

We used 207 meteorological stations, which recorded mean precipitation rates (pr) between  $1972.5 \pm 18.3$  and  $2017.0 \pm 13.62$ . For the subsequent analyses, we only used the observations within the period 1979–2013 to match CHELSA v1.2. The data of these stations were checked for errors in locations or in observations. Specifically, we removed four stations that were considered extreme outliers by showing >10 times higher observed precipitation rates than the modelled ones by CHELSA v1.2.

The bias correction using station data followed the methodology described by Karger et al. (2021). In a first step, the bias between observed monthly precipitation rates at meteorological stations  $pr_{obs}$  and the model based on monthly precipitation rates  $pr_{mod}$  from CHELSA v1.2 is calculated as the ratio:

$$R_{mod}^{obs} = \frac{pr_{obs} + c}{pr_{mod} + c}$$

with  $c$  being a constant of  $0.01 \text{ kg m}^{-2} \text{ month}^{-1}$  to avoid division by zero. The resulting point data are then spatially interpolated using a multi-level B-spline interpolation (Lee et al., 1997) with 14 error levels and optimized using a B-spline refinement to a horizontal resolution of 30 arc-seconds (hereafter ~1 km). This multilevel B-spline approximation  $S$  (Lee et al., 1997) applies a B-spline approximation to  $R_m$  starting with a coarsest grid  $\phi_0$  from a total set of 14 control grids  $\phi_0, \phi_1, \phi_2, \dots, \phi_n$  with  $n=14$  that have been generated using optimized B-spline refinement (Press et al., 1989). The resulting B-spline function:

$$f_0(R_{mod}^{obs})$$

gives the first spatial approximation of the model bias  $R$ . However,  $f_0(R_{mod}^{obs})$  leaves a first deviation  $\Delta^1 R_{mod}^{obs}$  between interpolated values at the control grid and  $R_{mod}^{obs}$  being:

$$\Delta^1 R_{mod}^{obs} = R_{mod}^{obs} - f_0(x_c, y_c)$$

at each grid cell location  $(x_c, y_c, R_{mod}^{obs})$ . Then the next control grid  $\phi_1$  is used to approximate  $f_1(\Delta^1 R_{mod}^{obs})$ . This approximation is then repeated  $n$  times on the sum of

$$f_0 + f_1 = R_{mod}^{obs} - f_0(x_c, y_c) - f_1(x_c, y_c)$$

at each grid cell  $(x_c, y_c, R_{mod}^{obs})$  resulting in the gap free interpolated bias surface  $R_{int}$  (Press et al., 1989). The bias corrected precipitation at 1 km resolution is then calculated using:

$$pr_c^{cor} = pr_{mod} \times R_{int}$$

### 2.2.2 | Boundary layer height adjusted downscaling of monthly precipitation rates

A main driver of precipitation gradients is the mesoscale orographic configuration that can induce precipitation by the lifting

and cooling of air masses over topographically complex terrain. Both the CHELSA v1.2 data and the station measurements do already include these effects. Orography, however, still affects precipitation rates at very fine scales that are hidden by their coarse resolution. In the Canary Islands, for example, clouds often form at mid elevations, leaving the high elevations cloud free. Additionally, below the clouds, fine-scale orography does not influence precipitation rates anymore, as rain clouds usually have a size larger than 1 km. To correct for this elevation-dependent effect, we included a boundary layer height correction of precipitation rates in the downscaling (Karger et al., 2017, 2020). We used the boundary layer height planetary boundary layer (PBL) from the ERA-Interim climate data set, a global atmospheric reanalysis produced by the European Centre for Medium-Range Weather Forecasts (Dee et al., 2011). PBL is then used to calculate the distance of the orography to the boundary layer  $\Delta z$  by

$$\Delta z = \text{PBL} - z$$

And further adjusted by:

$$\Delta z_h^{\text{cor}} = \begin{cases} 0, z < \text{PBL} \\ d^{\left(\frac{\Delta z - \Delta z_{\text{min}}}{\Delta z_{\text{max}} - \Delta z_{\text{min}}}\right)}, z \geq \text{PBL} \end{cases}$$

where the exponent of  $d$  represents the scaled high-resolution orography using  $\Delta z_{\text{max}}$  being the maximum distance to the boundary layer and  $\Delta z_{\text{min}}$  the minimum distance to the boundary layer. The parameter  $d$  is a tuning parameter that has been adjusted based on the fit of the subsequent downscaling using a sensitivity analysis (Figure S2) and set to a value of 100. It adjusts the strength of the orographic terrain effect of precipitation below the boundary layer using a logarithmic function. The high-resolution precipitation rates at coarse resolution  $\text{pr}_c^{\text{cor}}$  are then calculated using:

$$\text{pr}_h = \text{pr}_c^{\text{cor}} \frac{(z_h + (S(z_c) - z_h)(1 - \Delta z_h^{\text{cor}}))}{S(z_c)}$$

where  $z_h$  is the orography at 5 m resolution,  $z_c$  is the orography at 1 km resolution B-spline interpolated ( $S$ ) to 5 m resolution.

### 2.2.3 | Temperature downscaling

We used 101 meteorological stations, which recorded mean maximum and minimum near-surface 2-m air-temperature (tasmx, tasmin) between  $1986.6 \pm 17.2$  and  $2011.4 \pm 13.6$ . For the subsequent analyses, we only used the observations within the period 1979–2013. The data of these stations were checked for errors in locations or in observations. We only used stations with a minimum of 10 years of records.

We used a lapse-rate based downscaling of temperatures following the methodology of Karger et al. (2017). We calculated monthly mean temperature lapse rates from ERA-Interim for the

period 1979–2013 based on a linear regression between temperatures and geopotential heights at all pressure levels from 1000 to 300 hPa from ERA-Interim. As lapse rate  $\Gamma$  we used the parameter estimate of the regression for temperature. The lapse rate has then been B-spline interpolated to a 5-m resolution. The grid elevation at 1-km resolution and the station elevation can deviate substantially due to differences in spatial resolution. To account for this potential artefact, we corrected the temperature measured at the station with the elevational difference  $\Delta z$  between the 1-km grid cell elevation from GMTED2010 (Danielson & Gesch, 2011) and the elevation of the meteorological station, as well as the lapse rate  $\Gamma$  by using:

$$\text{tasmx}_{\text{obs}}^{\text{cor}} = \text{tasmx}_{\text{obs}} + (\Delta z \cdot \Gamma)$$

and:

$$\text{tasmin}_{\text{obs}}^{\text{cor}} = \text{tasmin}_{\text{obs}} + (\Delta z \cdot \Gamma)$$

The bias  $R_{\text{int}}$  has then been calculated in the exact same way as for precipitation. At the 1-km resolution the bias corrected maximum and minimum near-surface 2-m air-temperatures have then been calculated by:

$$\text{tasmx}_c^{\text{cor}} = \text{tasmx}_{\text{mod}} \times R_{\text{int}}$$

and:

$$\text{tasmin}_c^{\text{cor}} = \text{tasmin}_{\text{mod}} \times R_{\text{int}}$$

And further downscaled to 5 m resolution using:

$$\text{tasmx}_h = S(\text{tasmx}_c^{\text{cor}}) + ((S(z_c) - z_h) \cdot \Gamma)$$

and:

$$\text{tasmin}_h = S(\text{tasmin}_c^{\text{cor}}) + ((S(z_c) - z_h) \cdot \Gamma)$$

where  $S$  denotes a B-spline interpolation,  $z_h$  is the orography at 5 m resolution,  $z_c$  is the orography at 1 km resolution.

### 2.2.4 | Statistical validation of CanaryClim

Bias correction of CanaryClim variables was validated using a 10-fold cross validation with 10 iterations that randomly removes one-fold of the data as test and leaves ninefolds as training. We then repeated the bias correction for temperature and precipitation using the training data and tested the resulting climatological surfaces using the test set of stations for several metrics.

We used the correlation between a simulated data set ( $x_{\text{sim}}$ ), such as the downscaled precipitation or temperature surfaces, with the values observed at meteorological stations ( $x_{\text{obs}}$ ) that overlap with a grid cell of the simulated data set. The correlation is calculated based on Pearson's correlation coefficient,

$$\rho = \frac{\text{COV}(x_{\text{sim}}, x_{\text{obs}})}{\sigma(x_{\text{sim}})\sigma(x_{\text{obs}})}$$

where  $x_{\text{obs}}$  represents the observed time series at a meteorological station  $x_{\text{sim}}$  the downscaled timeseries, cov the covariance, and  $\sigma$  the

standard deviation. Additionally, we used root mean squared error (RMSE) defined as:

$$\text{RMSE} = \sqrt{\frac{1}{n} \left( \sum_{i=0}^n (x_{\text{sim}_i} - x_{\text{obs}_i})^2 \right)}$$

where  $n$  is the number of time steps of a timeseries. Furthermore, the mean absolute error (MAE) was computed according to:

$$\text{MAE} = \frac{1}{n} \left( \sum_{i=0}^n |x_{\text{sim}_i} - x_{\text{obs}_i}| \right)$$

Additionally, we used the Kling–Gupta efficiency (KGE) to calculate a combined score based on the bias component  $\beta$ , the ratio of estimated and observed means, and the variability component  $\gamma$  by the ratio of the estimated and observed coefficients of variation:

$$\text{KGE} = 1 - \sqrt{(r-1)^2 + (\beta-1)^2 + (\gamma-1)^2}$$

where:

$$\beta = \frac{\mu_{\text{sim}}}{\mu_{\text{obs}}} \text{ and } \gamma = \frac{\frac{\sigma_{\text{sim}}}{\mu_{\text{sim}}}}{\frac{\sigma_{\text{obs}}}{\mu_{\text{obs}}}}$$

KGE,  $r$ ,  $\beta$ , and  $\gamma$  values all have their optimum at 1. KGE values between  $-0.41$  and  $1$  indicate that the model estimates are better than just taking the mean of the observations (Knoben et al., 2019).

## 2.2.5 | Future climate variables

As the present periods of CHELSA v.2.1 (1981–2010) and CanaryClim v1.0 (1979–2013) slightly differs, we first generated present (1979–2013) and future (2071–2100) maps at 1-km resolution in the Canary Islands for monthly minimum, maximum and mean temperatures and monthly amount of precipitation using the `chelsea_cmip6` algorithm available at [https://gitlabext.wsl.ch/karger/chelsea\\_cmip6](https://gitlabext.wsl.ch/karger/chelsea_cmip6) (Karger et al., 2023). This step was performed for five Earth system models, which show different levels climate sensitivity and, therefore, the amount of global surface warming that will occur in response to a rising of atmospheric  $\text{CO}_2$  concentrations (Tokarska et al., 2020). This step is relevant because it allows us to avoid bias in the analysis results towards a certain climate model (Hemer et al., 2013). From higher to lower climate sensitivity, we selected UKESM1-0-LL, IPSL-CM6A-LR, GFDL-ESM4, MRI-ESM2-0 and MPI-ESM1-2-LR. Each model was associated with three shared socio-economic pathways (hereafter termed as SSP): SSP1-2.6, SSP 3–7.0 and SSP 5–8.5 (Table S2). These three SSPs provide contrasted projected socio-economic global changes in the near future, under which the global mean temperature changes will range from approximately  $1.5$ – $5^\circ\text{C}$  in 2100 (O'Neill et al., 2016). From a different angle, these three SSP scenarios represent the low, medium and high range of future forcing pathways, implementing radiative forcing levels of 2.6, 7.0 and  $9.5 \text{ Wm}^{-2}$  in 2100 (O'Neill et al., 2016).

Then, we calculated the anomaly ( $\Delta$ ) between the 1979 and 2013 present reference period (ref) and the 2071–2100 future period (fut)

for a given variable at the spatial resolution of the climate model (Arnell et al., 2001). For mean daily 100-m air temperatures (tas), as well as daily maximum (tasmax) and minimum (tasmin) 100 m air temperatures, a delta change method is applied so that the anomaly is given by:

$$\Delta \text{tas}_{\text{fut}}^{\text{ref}} = \text{tas}_{\text{low}}^{\text{ref}} - \text{tas}_{\text{low}}^{\text{fut}}$$

This calculation is performed at a 1-km resolution (low). The anomaly  $\Delta \text{tas}_{\text{fut}}^{\text{ref}}$  is then interpolated to the spatial resolution of the high-resolution (high) reference climatology using a cubic-spline interpolation (CS) (Hall & Meyer, 1976) and subtracted to the high resolution reference climatology ( $\text{tas}_{\text{high}}^{\text{ref}}$ ), so that:

$$\text{tas}_{\text{high}}^{\text{fut}} = \text{tas}_{\text{high}}^{\text{ref}} - \text{CS}(\Delta \text{tas}_{\text{fut}}^{\text{ref}})$$

The same applies for tasmax and tasmin. This calculation is made separately for each month from January to December. For precipitation (pr), an additive delta change method can potentially generate negative values. To derive anomalies, we used a reduction method, and adding a constant  $c$  of  $10^{-7} \text{ kgm}^{-2} \text{ day}^{-1}$  to both the reference and the future data to avoid division by zero:

$$\Delta \text{pr}_{\text{fut}}^{\text{ref}} = \frac{\text{pr}_{\text{low}}^{\text{ref}} + c}{\text{pr}_{\text{low}}^{\text{fut}} + c}$$

As for temperature, the anomalies are then interpolated using a cubic-spline interpolation to a 1 km resolution and divided to a high-resolution reference climatology using:

$$\text{pr}_{\text{high}}^{\text{fut}} = \left( \frac{\text{pr}_{\text{high}}^{\text{ref}} + c}{\text{CS}(\Delta \text{pr}_{\text{fut}}^{\text{ref}})} \right) - c$$

The delta change method as applied here is relatively insensitive regarding individual model bias of the climate model used, as it only uses the difference (ratio) for a given variable between a reference period and a future period. Following the definitions of CHELSA (Karger et al., 2017, 2023), the 19 CanaryClim bioclimatic variables (BIO1–BIO19) were then generated using SAGA-GIS.

## 2.3 | Topographic variables

To generate topographic variables using the software SAGA-GIS v.7.9.1, digital elevation maps (DEM) of the Canary Islands were downloaded at 2-m resolution from IGN (<https://martingonzalez.net/ign-dem-grabber/>). Slope, aspect and five types of curvatures were generated at 2-m resolution via the method of 9 parameter second-order polynomial (Zevenbergen & Thorne, 1987). The aspect map was then decomposed into two axes: North–South (northernness) and East–West (easterness), which correspond to the cosine and sine of the aspect, respectively. The topographic wetness index (TWI) with the related catchment area and slopes were computed at

2-m resolution via the 'TWI' module (Beven & Kirkby, 1979; Böhner & Selige, 2006; Moore et al., 1991; Zevenbergen & Thorne, 1987). All the topographic variables were afterwards resampled to 100 m (EPSG:32628; extent: 183,460 m, 3,057,114 m; 655,860 m, 3,255,114 m [xmin, ymin; xmax, ymax]) and 30 arc-seconds (~1 km; EPSG: 4326; extent: -20°, 27°; -12°, 30° [xmin, ymin; xmax, ymax]) resolution applying a mean via the "terra" R package (Hijmans, 2022). This strategy was performed to match the resolutions of both climatic data sets (CanaryClim vs. CHELSA). The final list of topographic variables generated are presented in Table S3.

## 2.4 | Selecting environmental climatic variables for species distribution modelling

In order to avoid multicollinearity, we computed Pearson's correlation coefficient in the 'terra' R package among all the climatic and topographic variables considered (Table S3) to identify highly correlated variables ( $|r| > 0.7$ ) at 100-m resolution (Dormann et al., 2013; Guisan et al., 2017; Zurell et al., 2020). We kept the eight following present time variables: BIO1 (mean annual air temperature, °C), BIO2 (mean diurnal air temperature range, °C), BIO12 (annual precipitation amount, kg m<sup>-2</sup>), BIO15 (precipitation seasonality, kg m<sup>-2</sup>), BIO18 (mean monthly precipitation amount of the warmest quarter, kg m<sup>-2</sup>), TWI, northerness, and easternness; for performance comparison purposes, the same variables were selected from CHELSA data set. Inclusion of the variables related to precipitation (i.e. BIO12, BIO15, BIO18) and relative humidity (i.e. TWI, northerness, easternness) is supported by the importance of water availability for bryophytes due to their poikilohydric condition (Patiño et al., 2022; Patiño & Vanderpoorten, 2018) and, in particular, for the bryophyte flora endemic to Macaronesia due to its overall affinity for montane cloud forests (Patiño et al., 2014; Vanderpoorten et al., 2011). BIO1 and BIO2 can further contribute to control for the relevance of high temperatures on mortality rates in temperate and subtropical bryophytes (He et al., 2016; Patiño et al., 2016; Patiño & Vanderpoorten, 2018).

## 2.5 | Modelling approach: Ensemble of small models

Assumptions underlying our species distribution models are described in Table S4 according to Zurell et al. (2020). Independent models were generated using the selected CanaryClim and CHELSA variables at 100-m and 1-km resolution, respectively, together with the selected topographic variables as predictors. As we had between 10 and 100 occurrences per species, we employed 'ensemble of small models' (ESMs), which have been specifically developed for small data sets (Breiner et al., 2015, 2018; Erickson & Smith, 2023; Lomba et al., 2010); ESMs have been successfully implemented in bryophytes in recent studies (Cerrejón et al., 2022; Collart, Hedenäs

et al., 2021). Ensemble of small models consist in generating bivariate models with all possible pairs of predictors, which are subsequently combined into an ensemble. Such an approach thus avoids overfitting without losing explanatory power (Breiner et al., 2015). Based on the recommendations provided by Breiner et al. (2015), we employed Gradient Boosting Machine (Jerome, 2001) with the default parameters in 'ecospat' R package (Broennimann et al., 2022). Models were calibrated from the species occurrence data and 10,000 background points randomly selected in the Canary Islands with the 'sp' R package (Bivand et al., 2008; Pebesma & Bivand, 2005). Species occurrences and background points were equally weighted, and the latter were kept constant for the modelling at the two spatial resolutions.

We generated species response curves for each environmental variable using the 'ecospat' R package (Broennimann et al., 2022) by projecting all bivariate models, successively keeping one variable and setting the other ones at their median values. The resulting probabilities were then combined into an ensemble and plotted to obtain the mentioned response curves.

Models were then evaluated from 10 replicates of 28 bivariate models. In each replicate, 70% of the data were used for model training (training set) and the remaining 30% for model testing (test set). Bivariate models were afterwards combined together, applying a weighted mean based on their Somer's *D* values ( $2 \times \text{AUC} - 1$ ) and removing models with a Somer's *D* lower or equal to 0. Model accuracy was assessed by pooling the suitability values from the 10 test sets to obtain an independent series of suitability values with roughly the same size as the initial data set, as recommended by Collart and Guisan (2023). We measured model accuracy using the Boyce Index, which was designed for presence-only data. Although AUC and MaxTSS require presence-absence data and can be misleading with presence-only data sets (Leroy et al., 2018), we also computed them for comparison purpose because they remain the most widely used metrics (Guisan et al., 2017).

Models were projected under present (1979–2013) and future (2071–2100) climate conditions. For the future, we used two out of the five individual model intercomparison projects included in the CanaryClim data set and the three SSPs. The selected global circulations models were UKESM1-0-LL (hereafter UKESM) and GFDL-ESM4 (hereafter GFDL), which correspond to high and low climate sensitivity, respectively (Lange, 2019, 2021). These two projects resulted to be the most distant ones regarding their quartiles (minimum, first quartile, median, third quartile and maximum values across the 19 bioclimatic variables and the three SSPs (Figure S3 and Tables S5 and S6).

The resulting habitat suitability maps were binarized using the threshold that maximizes the TSS, as recommended by Liu et al. (2013). Percentages of lost and gained probably suitable pixels in 2071–2100 compared to present time were computed using the 'biomod2' R package (Thuiller et al., 2022). To compare the outputs obtained using CanaryClim and CHELSA, the binarized maps obtained with CanaryClim were aggregated to reach the same

resolution as CHELSA. A 1-km pixel was thus considered probably suitable if at least one of its 100 m constitutive pixels was considered as such. Because binarization represents a loss of information and is uncertain in the context of presence-only data (Leroy et al., 2018; Santini et al., 2021), we complemented it by producing histograms of suitability values obtained with CanaryClim and CHELSA-based models. In particular, we compared suitability histograms between present and future conditions and histograms of future suitability with CanaryClim and CHELSA, respectively.

### 3 | RESULTS

The high-resolution climate data set, CanaryClim v1.0 and the topography data set, both generated in the present study are available at <https://doi.org/10.6084/m9.figshare.22060340> and <https://doi.org/10.6084/m9.figshare.22060433>, respectively.

#### 3.1 | Present and future climate data sets

The climate model performances are available in Tables S7 and S8. The mean correlations between the predicted climate and weather stations measurements were on average  $0.74 \pm 0.22$ ,  $0.85 \pm 0.05$  and  $0.82 \pm 0.07$  for maximal monthly temperature, minimal monthly temperature and monthly precipitation, respectively. General patterns in temperature and precipitation between CHELSA and CanaryClim data sets showed relevant differences across space and time. Under present conditions, annual mean temperature varied, on average, from  $17.8 \pm 3.2^\circ\text{C}$  to  $19.3 \pm 2.9^\circ\text{C}$ , with CHELSA predicting colder temperatures than CanaryClim. Annual precipitation showed important differences, with an average across pixels of  $245.6 \pm 133.8$  mm in CHELSA versus  $300.1 \pm 209.3$  mm in CanaryClim. When scanning all 1-km pixels, a difference of up to 59 mm was observed between the value predicted by CanaryClim in the wettest 100 m constitutive pixel and CHELSA. These temperature and precipitation discrepancies were mostly located in northern slopes and montane ridges, as the example represented in Figure 2 for the Anaga Peninsula in Tenerife island (Figure S4).

On average, predicted annual mean temperature increase in 2100 was higher with CanaryClim than CHELSA data set. Specifically, under the warming scenarios SSP 1–2.6, SSP 3–7.0 and SSP 5–8.5 and the GFDL (UKESM) global circulations models, we predicted average temperature increases with CHELSA of  $0.9 \pm 0.05^\circ\text{C}$  ( $1.8 \pm 0.2^\circ\text{C}$ ),  $2.2 \pm 0.06^\circ\text{C}$  ( $3.3 \pm 0.2^\circ\text{C}$ ), and  $2.3 \pm 0.06^\circ\text{C}$  ( $4.1 \pm 0.2^\circ\text{C}$ ) (Figure S3). With CanaryClim, these values were  $1.2 \pm 0.02^\circ\text{C}$  ( $2.2 \pm 0.04^\circ\text{C}$ ),  $2.4 \pm 0.01^\circ\text{C}$  ( $4.0 \pm 0.05^\circ\text{C}$ ), and  $2.9 \pm 0.01^\circ\text{C}$  ( $4.7 \pm 0.04^\circ\text{C}$ ), respectively. For annual precipitation, a higher decrease in 2100 was predicted by CHELSA compared with CanaryClim (Figure S3). The resulting ratios (i.e., future precipitation/present precipitation) when future and present precipitation regimes were estimated and compared ranged on average from  $1.03 \pm 0.02$  to  $0.91 \pm 0.02$  in CanaryClim and from  $1.00 \pm 0.03$  to  $0.82 \pm 0.01$  in CHELSA (Figure S4).

#### 3.2 | Present and future species distribution predictions

Species distribution prediction maps are available at <https://doi.org/10.6084/m9.figshare.22776545>. Based on CHELSA and CanaryClim data as predictors, SDMs exhibited similar accuracy (average CHELSA SDM Boyce Index =  $0.866 \pm 0.129$ , average CanaryClim SDM Boyce Index =  $0.854 \pm 0.106$  across species; Figure 3). Although all the species had AUC values  $>0.8$ , two and six species showed Boyce index  $<0.8$  and, seven and nine showed MaxTSS  $<0.8$  for CHELSA and CanaryClim SDMs, respectively (Table S9). In addition, response curves were relatively similar between CHELSA and CanaryClim SDMs across species (Figure S5), at least for species with similar ecological requirements. For instance, montane cloud laurel forest species tended to exhibit alike response curves compared with the only alpine species in our study, *G. curviseta*. In addition, response curves seemed to display certain levels of overfitting, particularly for precipitation variables (Figure S5).

The percentage of exclusive 1-km-resolution pixels predicted by CanaryClim or CHELSA SDMs as likely suitable environmentally reached 55.9% and 21.9%, respectively (Figure 4 and Table S10). Only 22.2% of the pixels were in common to the two climatic SDMs under present conditions. These differences in environmentally (likely) suitable areas are even more pronounced when SDMs were projected onto future climatic layers. Specifically, 79.8%–99.3% of all pixels identified as likely suitable by either CanaryClim or CHELSA models were exclusive to the former (Figure 4 and Table S10). The percentage of probably suitable pixels exclusively predicted by CHELSA or predicted by the two climate data sets only reached 0.04%–11.9% and 0.01%–8.3%, respectively (Figure 4 and Table S10).

There was a further, strong spatial discrepancy between the projections generated with CanaryClim and CHELSA SDMs. The proportion of pixels predicted to become likely suitable in 2100 as compared to the present was substantially higher with CanaryClim (8.1%–28.3% depending on climate change scenarios) than with CHELSA (0.0%–2.7%) models (Figure 5). These patterns based on binarized suitability maps were mirrored by the distributions of suitability values at time present and in 2100, with higher proportions of pixels with high suitability values obtained under present conditions than in 2100 (Figure S6). Regarding the loss of probably suitable range, CanaryClim and CHELSA predictions were globally more similar, with high rates of predicted loss of the probably suitable range at present time, reaching between 70.6% and 96.0% across species for CanaryClim and between 68.6% and 99.7% for CHELSA (Figure 5).

This trend was only partially reflected by the distribution of suitability values in 2100, with higher suitability values with CanaryClim (suitability averaged across pixels:  $0.105 \pm 0.056$ – $0.113 \pm 0.06$  depending on future scenarios) than with CHELSA ( $0.054 \pm 0.045$ – $0.064 \pm 0.051$ ) (Figure S6). Moreover, these differences, in suitability change between present and future, were not consistent across all



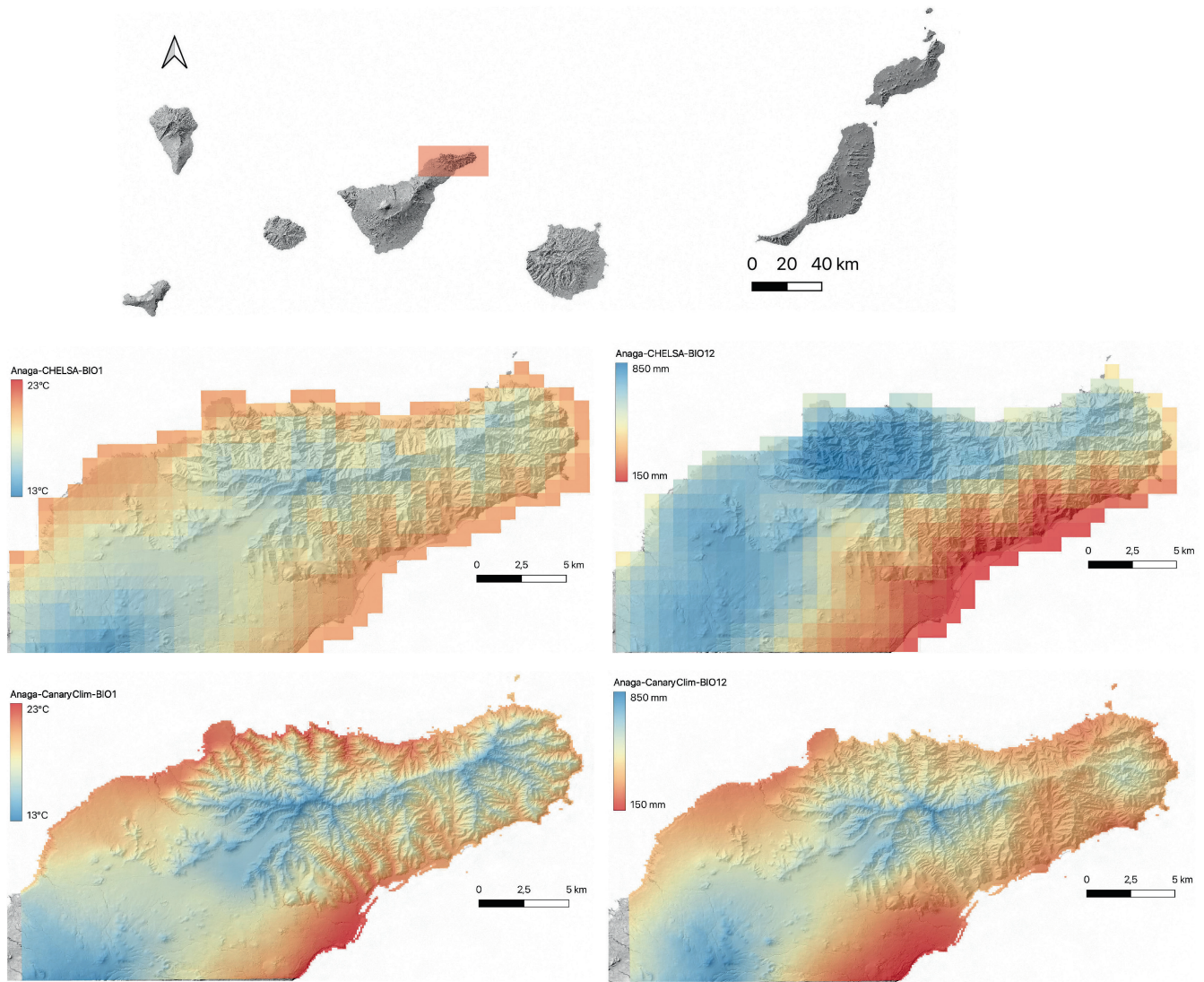


**FIGURE 2** Comparison of mean annual air temperature (BIO1; left panels) and annual precipitation amount (BIO12; right panels) from 1979 to 2013 predicted from two climatic datasets with different resolutions (~1 km in CHELSA and 100 m in CanaryClim). Values are provided for the Anaga Peninsula (Tenerife, Canary Islands) as an example.

the species (Table S11). As an example, >99% of the current potential distribution range was predicted to become probably unsuitable for four species under the GFDL 5–8.5 scenario in CanaryClim, while the number reaches 12 out of 14 species in CHELSA. In fact, a number of species showed high probability of persistence in small areas across mid-elevation ridges with CanaryClim SDMs, but not with CHELSA SDMs (Figures 6, S7 and S8). Among these species, *C. longisetus*, *E. intermedia*, *F. polysticta*, *L. canariensis* or *R. pseudolitorea* matched the commented pattern under CanaryClim, while we only found persisting areas under CHELSA models for *E. intermedia* (Figures 6, S7 and S8).

Using CHELSA, no likely suitable pixels remain in 2100 for 3–11 species depending on the scenario implemented (Table S11). With CanaryClim SDMs, none of the studied species was predicted to lose all their suitable pixels in the future under the scenario GFDL 1–2.6, no likely suitable pixels remain suitable for one species with

the scenarios GFDL 3–7.0, UKESM 1–2.6 and 3–7.0, and for two species with the scenario UKESM 5–8.5 (Table S11). Under the UKESM 5–8.5 scenario, the predicted loss of suitable range tended to be worse, reaching at least 99% in six and 10 species with CanaryClim and CHELSA models, respectively (Table S11).

## 4 | DISCUSSION

Our study demonstrates the importance of considering high-resolution climate data sets to forecast climate change responses of small plants and identify potential future climate microrefugia and range expansion across areas that might become climatically suitable in the near future (Patiño et al., 2022). We further showed that SDMs projected at fine-scale resolution do not necessarily lead to better model accuracy.

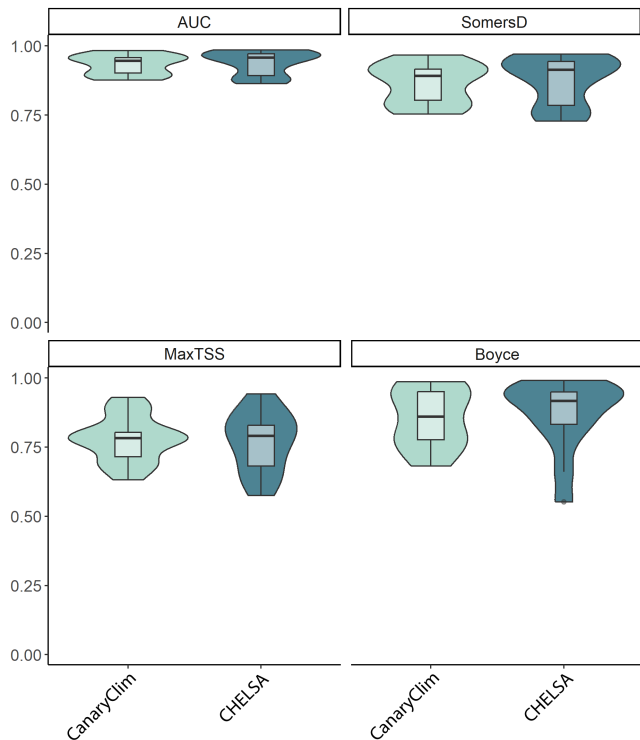


**FIGURE 3** Distribution and boxplots of performances for the ensemble small models realized using data at 100 m (CanaryClim) and ~1 km (CHELSA) resolutions. The boxplots show the 1st and 3rd quartiles (upper and lower bounds), 2nd quartile (centre), 1.5 × interquartile range (edges of the box).

#### 4.1 | Fine versus coarse-grain climate data sets

We showed that downscaling temperature and precipitation grids based on widely available climate station data can be envisioned as a reliable and advisable approach (Meineri & Hylander, 2017). Indeed, the downscaling approach performed well with noteworthy correlations between predicted and observed monthly amount of precipitation, minimum and maximal air temperature. However, we anticipate that these performances can be further improved by increasing the number of weather stations or by complementing the data using in situ microclimate measurements (Gril et al., 2023). From a topographical perspective, CanaryClim data provides temperature and precipitation estimates more strongly correlated with topography and aspect than what CHELSA data does, even when both data sets use digital elevation models to perform corrections (Karger et al., 2017). For instance, at the summit areas of the Anaga Peninsula in Tenerife (Figure 2), temperature and precipitation amounts are expected to reach the lowest and the highest values, respectively, in the region (del Arco-Aguilar & Rodríguez-Delgado, 2018; Marzol et al., 2011). This expectation seems to be better reproduced by the high resolution CanaryClim than the coarser-resolution CHELSA data set. This outcome is not unexpected as mounting literature has recently demonstrated the ability of downscaling climate data sets in order to reproduce fine-scale microclimatic gradients in mountain areas (Dobrowski, 2011; Lenoir et al., 2017).

On average, we found that CanaryClim predicts slightly higher temperatures and precipitations than CHELSA data set, under both present and future conditions. Since important differences in temperature and precipitation are explained by landscape physiography (Dobrowski, 2011; Dobrowski et al., 2009; Meineri et al., 2015), it seems reasonable to assume that coarser climatic data sets might experience limitations in identifying local ecological features that promote deviations from regional climatic patterns in rugged landscapes (Randin et al., 2009). Such a limitation can eventually homogenize the climatic gradients imposed by elevation, topography and slope, having a poor representation of rare microclimates (Moudry et al., 2023). This is in line with the idea that climatic conditions for a given pixel using databases at coarse resolution represent better the conditions that actually prevail at low rather than high elevation within that pixel. As proposed by Meineri and Hylander (2017), this phenomenon can have two complementary explanations. First, the available surface area often decreases with elevation (Elsen et al., 2020; Elsen & Tingley, 2015). Second, since different topographic factors are best represented at small grain size, the probability of representing environmental conditions of ridges decreases with increasing grain-size (Randin et al., 2009).

#### 4.2 | The potential and limitations of CanaryClim for modelling the impacts of a changing climate

In contrast to previous studies suggesting that increasing the resolution of climate data improves model performances (Chavier et al., 2022; Franklin et al., 2013; Manzoor et al., 2018; Meineri & Hylander, 2017), we did not find relevant differences in terms of model accuracy (Lembrechts, Lenoir et al., 2019; Stark & Fridley, 2022). This result suggests that: (i) spatial resolution of CanaryClim might not be sufficient to depict environmental gradients relevant to small organisms (Potter et al., 2013; Scherrer & Körner, 2010); (ii) apparent overfitted precipitation curves can generate uncertainty in the future predictions of bryophyte suitabilities (see Figure S5); and (iii) while microtopography and vegetation data can be important to predict bryophyte distribution (Cerrejón et al., 2020; Jiang et al., 2014), they cannot totally replace in situ measurements (Man et al., 2022). In this context, CanaryClim would be usefully complemented by field measurements of microclimate recorded with sensor networks (Bramer et al., 2018; Lembrechts & Lenoir, 2020) that, coupled with detailed information on topography and vegetation structure, can serve as complementary predictors of the climatic conditions prevailing at the level of microhabitats (e.g., Haesen et al., 2021). Since the networks and timespan of georeferenced microclimate stations remain limited, particularly for insular regions, such improvement calls for the need of long-term standardized microclimate sampling approaches (Lenoir et al., 2017; Patiño, Hedenäs et al., 2017; Patiño, Whittaker et al., 2017).

Despite the similar accuracy shown by CHELSA and CanaryClim SDMs, the use of either climate data set had substantial consequences on predictions of extinction risks in the Macaronesian

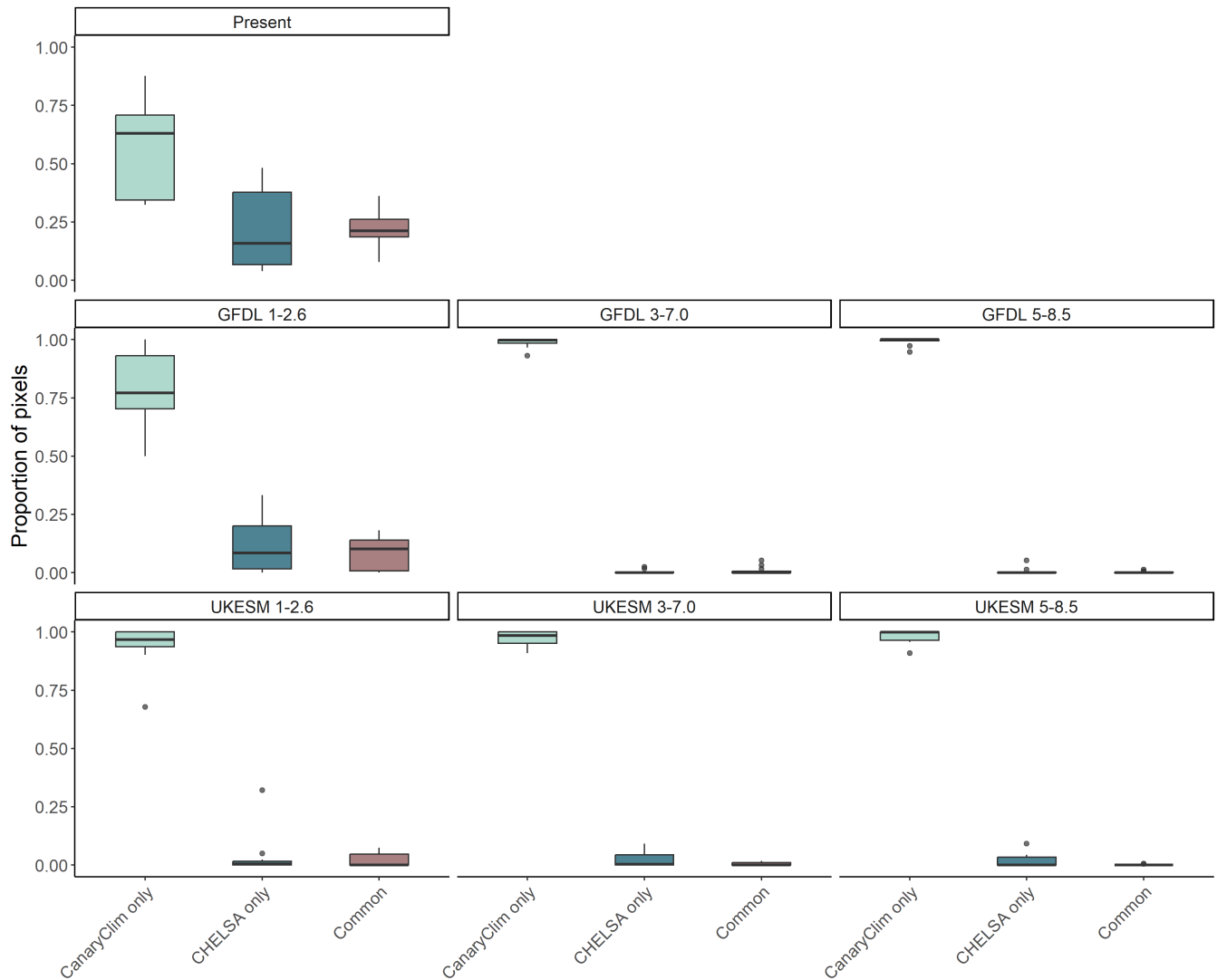


**FIGURE 4** Comparison of the proportion of 1 km resolution pixels becoming newly suitable in 2100 under two global circulation models (GFDL and UKESM) and three shared socio-economic pathways (SSP 1-2.6; 3-7.0; and 5-8.5) in 14 Macaronesian endemic bryophyte species across the Canary Islands, as predicted by species distributions models employing 100m (CanaryClim, a 1 km pixel being identified as suitable if a least one of its 100-m pixels are suitable) and ~1 km (CHELSA) resolution climatic data. The boxplots [showing the 1st and 3rd quartiles (upper and lower bounds), 2nd quartile (centre), 1.5× interquartile range (edges of the box), and extreme values (stars)] represent the proportion of suitable pixels with models based on CanaryClim only (light green), Chelsa only (blue), or both (red).

endemic bryophyte flora across the Canary Islands. This discrepancy originates from the much higher proportion of newly likely suitable pixels in 2100 predicted with CanaryClim, coupled with the substantial, but somewhat different predicted rate of loss of likely suitable range with both climatic data sets. Projections based on CHELSA and CanaryClim SDMs for 2100 had only 0.01%–8.3% of the newly likely suitable pixels in common, while 79.8% and 99.3% of the latter were identified by CanaryClim only. In turn, SDMs generated using CHELSA and CanaryClim both revealed substantial losses of probably suitable areas at present time. As an example, there were mosses such as *F. coacervatus*, *G. curviseta*, *L. treleasei* and *R. bourgaeana* and the liverworts *C. schaeferi* and *P. maderensis*, which were forecasted to probably become near extinct or vanished at the end of 21st century by the two climatic data sets (Table S10) and a former study using bioclimatic variables from WorldClim at the resolution of ~1 km (Patiño et al., 2016).

However, there are also important differences. First, despite response curves built with CanaryClim and CHELSA SDMs denote that both suffer from overfitting (Figure S5), it also seems that the high resolution CanaryClim data set does it to a lesser extent. Second, the overall number of species predicted to become extinct (i.e. a predicted total loss of all likely suitable pixels) in the near future was significantly lower under CanaryClim than CHELSA SDMs (Table S11) and the previous study based on classic SDMs (Patiño et al., 2016). Lastly, the projection of SDMs employing fine-grain CanaryClim compared with CHELSA data set revealed a higher number of microrefugia across mid-elevation ridges of the central and western Canarian islands. These areas are potentially dominated by montane cloud forests (del Arco-Aguilar et al., 2010; del Arco-Aguilar & Rodríguez-Delgado, 2018) and highly suitable for the Macaronesian endemic bryophyte assemblage (Patiño et al., 2014,

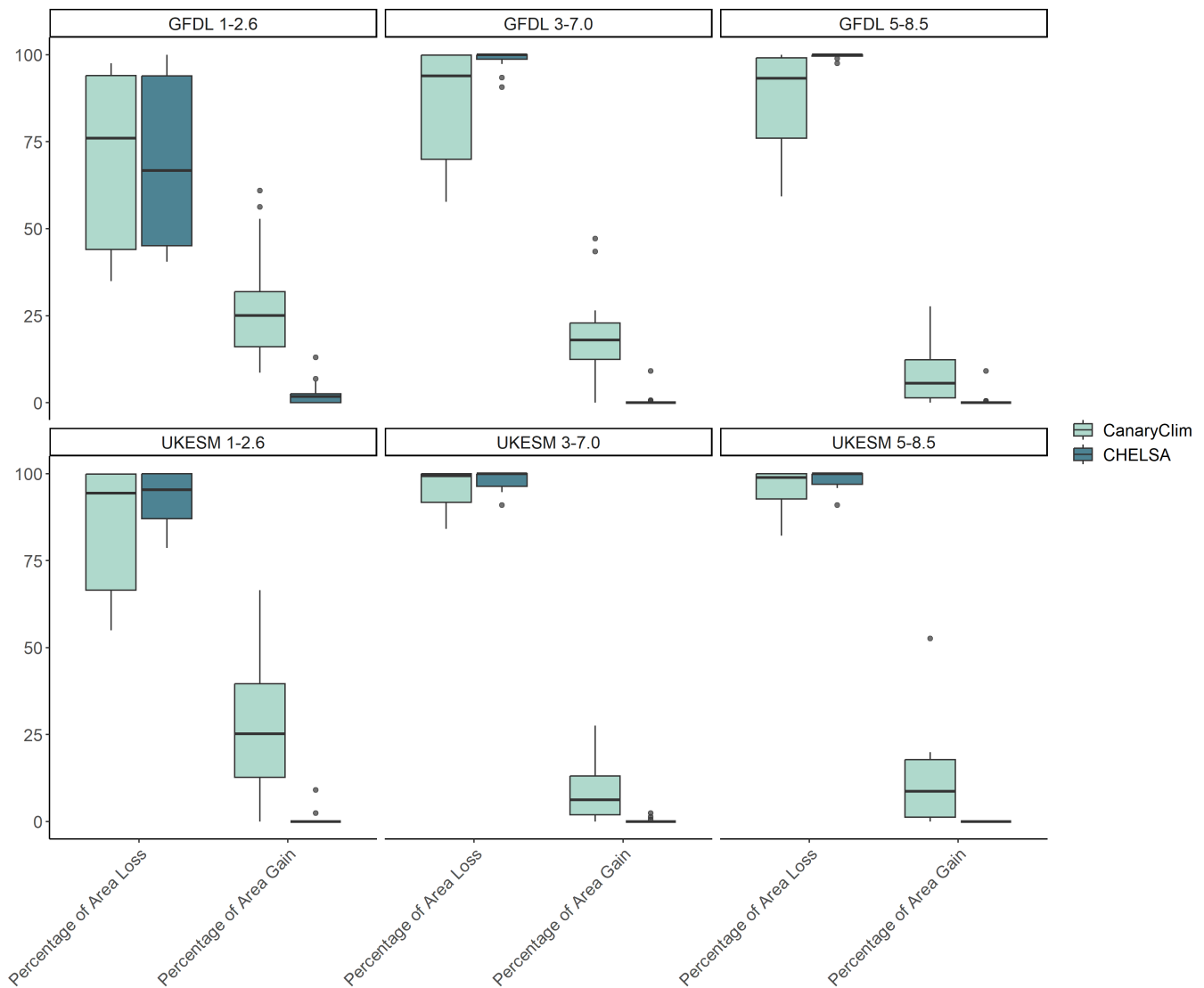


**FIGURE 5** Percentage of pixels becoming likely unsuitable or newly suitable in 2100 as compared to the present across 14 endemic bryophyte species across the Canary Islands, as predicted by the projection of species distribution models calibrated from climatic data at 100 m (CanaryClim) and ~1 km (CHELSA) resolutions. Analyses performed under two global circulation models (GFDL, UKESM) and three shared socio-economic pathways (1–2.6, 3–7.0, 5–8.5). Percentages are shown in boxplots, showing the 1st and 3rd quartiles (upper and lower bounds), 2nd quartile (centre),  $1.5 \times$  interquartile range (edges of the box), and extreme values (stars).

2016; Vanderpoorten et al., 2011). With the exception of *G. curviseta*, a species endemic to alpine areas of La Palma and Tenerife, the rest of the modelled species are mostly restricted to montane cloud forests. Since the bulk of the Macaronesian bryophyte endemic element is restricted to this ecosystem, it is not possible to draw conclusions about what would be the floristic element more threatened by climate change. Nevertheless, our findings support the idea that cloud montane species have a high extinction risk in a warmer and drier Canarian region (Patiño et al., 2016).

An additional potential limitation relies on the fact that our predictions did not consider biotic interactions, nor local adaptations, which can significantly impact the predicted range losses and gains (Guisan et al., 2017; Smith et al., 2019). Nonetheless, local adaptations are considered as rare for bryophytes as allopatric lineages can usually be explained by historical factors instead of niche

differentiation (Collart, Hedenäs et al., 2021; Hedenäs et al., 2022) and some evidence of niche conservatism has also been shown at the community level (Collart, Wang et al., 2021; Shen et al., 2022). In addition, niche expansion outside the native range was not demonstrated in invasive bryophyte species (Mateo et al., 2015).

From a conservation perspective, our findings suggest that the survival of the Macaronesian endemic bryophyte flora in the Canary Islands will greatly depend on its capacity to migrate into newly suitable areas. Such a dynamic scenario could, at first sight, seem compatible with the presumed high long-distance capacities of bryophytes (but see Zanatta et al., 2020). Our projections based on CanaryClim SDMs can therefore serve to identify and locate future, new key areas for bryophyte conservation, which in some cases are identified outside the current range of the Canarian montane cloud forest. Within this context, a key next step will be to validate the conservation value

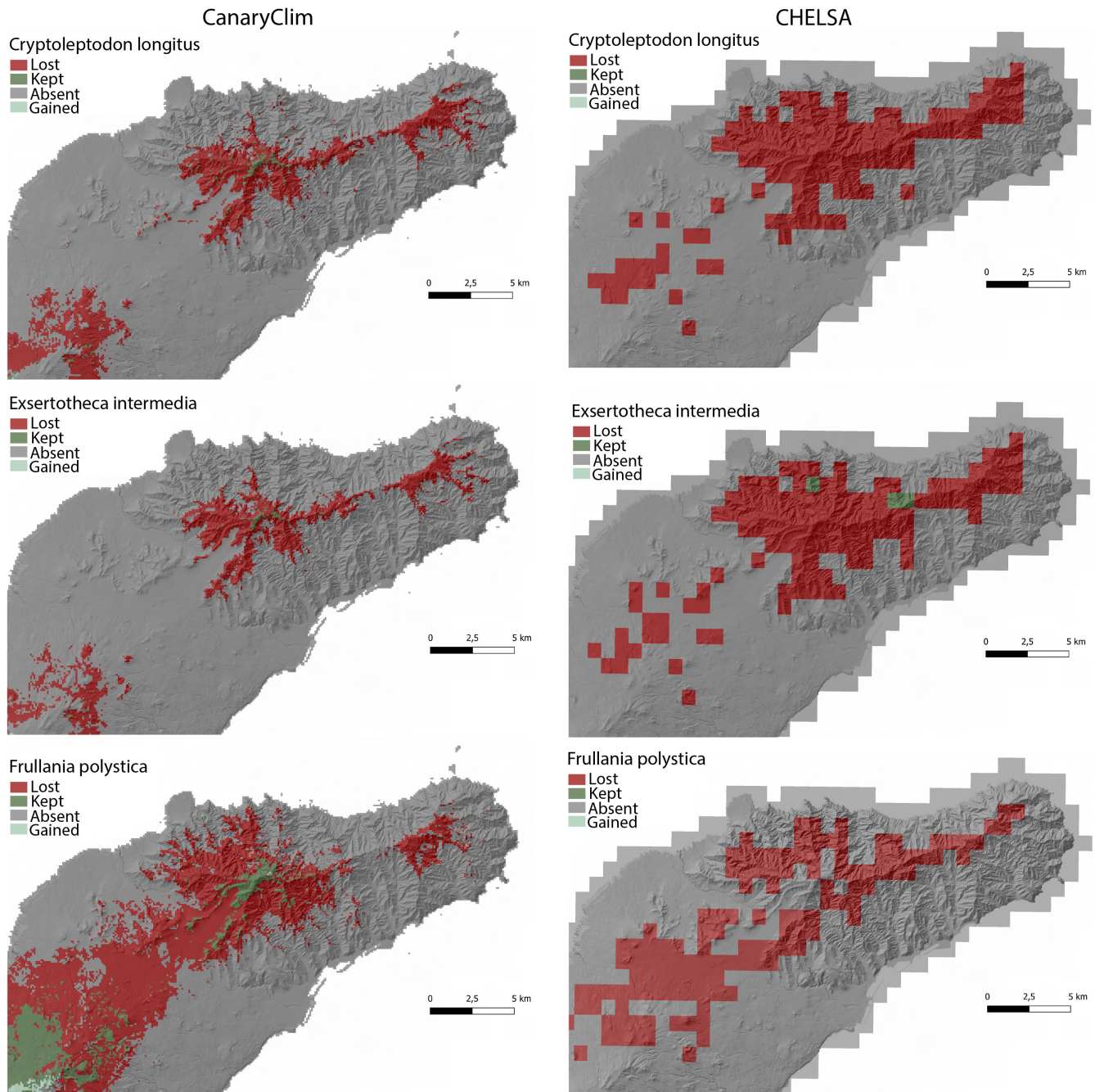


**FIGURE 6** Examples of potential microrefugia in Anaga Peninsula (Tenerife, Canary Islands). Lost, kept and gained climatically suitable areas for three Macaronesian bryophyte species in the Canary Islands under the GFDL 5–8.5 scenario are depicted. Stable habitat in CanaryClim (100 m) and CHELSA (~1 km) is mostly predicted at mid-elevation ridges. New climatically suitable ranges are mostly identified at higher elevations, but mainly by CanaryClim models. Absent denotes climatically unsuitable pixels under present and future conditions.

and viability of these putative areas to actually persist or play a role as microrefugia for the Macaronesian bryophyte flora under ongoing climate change (Finocchiaro et al., 2023; Greiser et al., 2020).

## 5 | CONCLUSIONS

The limited potential of island species to respond to climate change is of major concern to scientists, conservationists and

managers (Harter et al., 2015; Martín et al., 2012; Patiño, Whittaker et al., 2017). Our findings suggest that projections using climate data sets at different spatial resolution can lead to extremely different predictions at the local scale, reinforcing the need for caution when selecting the appropriate grain size in studies evaluating the potential impacts of climate change (Chauvier et al., 2022; Franklin et al., 2013; Guisan et al., 2007; Seo et al., 2008). This is reflected in the lower proportion of pixels becoming suitable in 2100 with CHELSA than CanaryClim SDMs, and the ability of the latter data

set to identify climatic microrefugia by 2100. We highlighted the potential of CanaryClim data set to fulfil key related tasks in order to: (i) improve impact evaluation of climate change and make predictions of species distributions at spatial scales that are actually relevant for conservation and management; (ii) identify suitable putative microrefugia and understand their dynamics; and (iii) revisit the level of protection of valuable sites to mitigate the loss of biodiversity. More specifically, CanaryClim SDMs predicted much larger buffered warming trends in mid-elevation ridges than the SDMs performed using CHELSA data set. Despite these differences and the fact that CanaryClim is restricted to the Canary Islands, the probability of becoming extinct was relatively similar with CHELSA and CanaryClim data sets only for a few species. This outcome supports the relevance of global data sets such as CHELSA, but also highlights that modelling results might vary widely among species and geographic contexts when compared with finer resolution data sets.

Our study provides evidence to the relevance of developing fine resolution predictions under future climate change scenarios, by means of local meteorological station data, which can account for the effects of topography and landscape in complex oceanic islands. In practice, CanaryClim exemplifies the idea that finer climate predictors can reproduce better strong gradients of environmental complexity, wherein coarser environmental variables can often lead to an underrepresentation of rare environments (Moudrý et al., 2023). In conclusion, this study encourages the need of considering future climatic changes at finer spatial and temporal resolution, which will provide more robust and realistic SDM projections under future climate change scenarios.

#### ACKNOWLEDGEMENTS

We are grateful to Dr. Pablo Lucas Máyer Suárez for assistance during the compilation of meteorological station data. The authors also thank the regional institutions and administrations that provide climate station data for the Canary Islands, including the “Agencia Estatal de Meteorología” (AEMET) and “Instituto Canario de Investigaciones Agrarias” (ICIA), as well as “AgroCabildo”. No permits were needed to perform this study. We sincerely thank Boris Leroy and two anonymous reviewers for improving our manuscript with their insightful feedback.

#### FUNDING INFORMATION

This research was supported by the Fundación BBVA project (INVASION - PR19\_ECO\_0046), Ministerio para la Transición Ecológica y el Reto Demográfico (JUNIPERADAPT, 2941/2022) and the Spanish Ministry of Science and Innovation (MICINN) project (ASTERALIEN - PID2019-110538GA-I00). JP was funded by the MICINN through the Ramón y Cajal Program (RYC-2016-20506). FC was funded by a grant from the Swiss National Science Foundation (SNSF; Grant number 197777).

#### CONFLICT OF INTEREST STATEMENT

The authors have no relevant financial or non-financial interests to disclose.


#### DATA AVAILABILITY STATEMENT

The high-resolution climate data set, CanaryClim v1.0, is available at <https://doi.org/10.6084/m9.figshare.22060340>. The topography data set generated in the present study is available at <https://doi.org/10.6084/m9.figshare.22060433>. Relevant results are also shared, such as all the habitat suitability maps at <https://doi.org/10.6084/m9.figshare.22776545>, as well as, high resolution versions of all the figures (Figures S1–S8) included in the Supplementary Materials at <https://doi.org/10.6084/m9.figshare.22128458>.

#### ORCID

Jairo Patiño  <https://orcid.org/0000-0001-5532-166X>

Flavien Collart  <https://orcid.org/0000-0002-4342-5848>

José Luis Martin-Esquivel  <https://orcid.org/0000-0001-8984-3423>

[org/0000-0001-8984-3423](https://orcid.org/0000-0001-8984-3423)

Agustín Naranjo-Cigala  <https://orcid.org/0000-0001-8191-7344>

Dirk N. Karger  <https://orcid.org/0000-0001-7770-6229>

#### REFERENCES

- Arnell, N., Nigel, W., & Liv, C. (2001). Hydrology and water resources. In J. J. McCarthy, O. F. Canziani, N. A. Leary, D. J. Dokken, & K. S. White (Eds.), *IPCC climate change 2001: Impacts, adaptation and vulnerability, the third assessment report of working group II of the intergovernmental panel on climate change (IPCC)*. Cambridge University Press.
- Ashcroft, M. B., Gollan, J. R., Warton, D. I., & Ramp, D. (2012). A novel approach to quantify and locate potential microrefugia using topoclimate, climate stability, and isolation from the matrix. *Global Change Biology*, 18(6), 1866–1879. <https://doi.org/10.1111/j.1365-2486.2012.02661.x>
- Azevedo, E. B. D., Santos Pereira, L. S., & Itier, B. (1999). Modelling the local climate in Island environments: Water balance applications. *Agricultural Water Management*, 40(2), 393–403. [https://doi.org/10.1016/S0378-3774\(99\)00012-8](https://doi.org/10.1016/S0378-3774(99)00012-8)
- Bennett, K. D., & Provan, J. (2008). What do we mean by ‘refugia’? *Quaternary Science Reviews*, 27(27), 2449–2455. <https://doi.org/10.1016/j.quascirev.2008.08.019>
- Berio Fortini, L., Kaiser, L. R., Xue, L., & Wang, Y. (2022). Bioclimatic variables data set for baseline and future climate scenarios for climate change studies in Hawai‘i. *Data in Brief*, 45, 108572. <https://doi.org/10.1016/j.dib.2022.108572>
- Beven, K. J., & Kirkby, M. J. (1979). A physically based, variable contributing area model of basin hydrology/un modèle à base physique de zone d'appel variable de l'hydrologie du bassin versant. *Hydrological Sciences Bulletin*, 24(1), 43–69. <https://doi.org/10.1080/0262667909491834>
- Bivand, R. S., Pebesma, E. J., & Gómez-Rubio, V. (2008). *Applied spatial data analysis with R*. Springer.
- Böhner, J., & Selige, T. (2006). Spatial prediction of soil attributes using terrain analysis and climate regionalisation. In J. Boehner, K. R. McCloy, & J. Strobl (Eds.), *SAGA - Analyses and modelling applications* (Vol. 115, pp. 13–27). Goltze.
- Bramer, I., Anderson, B. J., Bennie, J., Bladon, A. J., De Frenne, P., Hemming, D., Hill, R. A., Kearney, M. R., Körner, C., Korstjens, A. H., Lenoir, J., & Gillingham, P. K. (2018). Chapter three – Advances in monitoring and modelling climate at ecologically relevant scales. In D. A. Bohan, A. J. Dumbrell, G. Woodward, & M. Jackson (Eds.), *Advances in ecological research* (Vol. 58, pp. 101–161). Academic Press.
- Breiner, F. T., Guisan, A., Bergamini, A., & Nobis, M. P. (2015). Overcoming limitations of modelling rare species by using ensembles of small models. *Methods in Ecology and Evolution*, 6(10), 1210–1218. <https://doi.org/10.1111/2041-210X.12403>

- Breiner, F. T., Nobis, M. P., Bergamini, A., & Guisan, A. (2018). Optimizing ensembles of small models for predicting the distribution of species with few occurrences. *Methods in Ecology and Evolution*, 9(4), 802–808. <https://doi.org/10.1111/2041-210X.12957>
- Broennimann, O., Di Cola, V., & Guisan, A. (2022). *Ecospat: Spatial ecology miscellaneous methods*. R package version 3.4. <http://www.unil.ch/ecospat/home/menuguid/ecospat-resources/tools.html>
- Brooks, T. M., Mittermeier, R. A., da Fonseca, G. A. B., Gerlach, J., Hoffmann, M., Lamoreux, J. F., Mittermeier, C. G., Pilgrim, J. D., & Rodrigues, A. S. L. (2006). Global biodiversity conservation priorities. *Science*, 313(5783), 58–61.
- Correjo, C., Valeria, O., Mansuy, N., Barbé, M., & Fenton, N. J. (2020). Predictive mapping of bryophyte richness patterns in boreal forests using species distribution models and remote sensing data. *Ecological Indicators*, 119, 106826. <https://doi.org/10.1016/j.ecoli.2020.106826>
- Correjo, C., Valeria, O., Muñoz, J., & Fenton, N. J. (2022). Small but visible: Predicting rare bryophyte distribution and richness patterns using remote sensing-based ensembles of small models. *PLoS One*, 17(1), e0260543. <https://doi.org/10.1371/journal.pone.0260543>
- Chauvier, Y., Descombes, P., Guéguen, M., Boulangeat, L., Thuiller, W., & Zimmermann, N. E. (2022). Resolution in species distribution models shapes spatial patterns of plant multifaceted diversity. *Ecography*, 2022(10), e05973. <https://doi.org/10.1111/ecog.05973>
- Collart, F., & Guisan, A. (2023). Small to train, small to test: Dealing with low sample size in model evaluation. *Ecological Informatics*, 75, 102106. <https://doi.org/10.1016/j.ecoinf.2023.102106>
- Collart, F., Hedenäs, L., Broennimann, O., Guisan, A., & Vanderpoorten, A. (2021). Intraspecific differentiation: Implications for niche and distribution modelling. *Journal of Biogeography*, 48(2), 415–426. <https://doi.org/10.1111/jbi.14009>
- Collart, F., Wang, J., Patiño, J., Hagborg, A., Söderström, L., Goffinet, B., Magain, N., Hardy, O. J., & Vanderpoorten, A. (2021). Macroclimatic structuring of spatial phylogenetic turnover in liverworts. *Ecography*, 44, 1474–1485. <https://doi.org/10.1111/ecog.05659>
- Connor, T., Hull, V., Viña, A., Shortridge, A., Tang, Y., Zhang, J., Wang, F., & Liu, J. (2018). Effects of grain size and niche breadth on species distribution modeling. *Ecography*, 41(8), 1270–1282. <https://doi.org/10.1111/ecog.03416>
- Cos, J., Doblas-Reyes, F., Jury, M., Marcos, R., Bretonnière, P. A., & Samsó, M. (2021). The Mediterranean climate change hotspot in the CMIP5 and CMIP6 projections. *Earth System Dynamics*, 2021, 1–26. <https://doi.org/10.5194/esd-2021-65>
- Danielson, J. J., & Gesch, D. B. (2011). *Global multi-resolution terrain elevation data 2010 (GMTED2010)*. <https://pubs.usgs.gov/of/2011/1073/>
- De Frenne, P., Lenoir, J., Luoto, M., Scheffers, B. R., Zellweger, F., Aalto, J., Ashcroft, M. B., Christiansen, D. M., Decocq, G., De Pauw, K., Govaert, S., & Hylander, K. (2021). Forest microclimates and climate change: Importance, drivers and future research agenda. *Global Change Biology*, 27(11), 2279–2297. <https://doi.org/10.1111/gcb.15569>
- Dee, D. P., Uppala, S. M., Simmons, A. J., Berrisford, P., Poli, P., Kobayashi, S., Andrae, U., Balmaseda, M. A., Balsamo, G., Bauer, D. P., Bechtold, P., & Vitart, F. (2011). The ERA-interim reanalysis: Configuration and performance of the data assimilation system. *Quarterly Journal of the Royal Meteorological Society*, 137(656), 553–597. <https://doi.org/10.1002/qj.828>
- del Arco-Aguilar, M.-J., González-González, R., Garzón-Machado, V., & Pizarro-Hernández, B. (2010). Actual and potential natural vegetation on the Canary Islands and its conservation status. *Biodiversity and Conservation*, 19(11), 3089–3140. <https://doi.org/10.1007/s10531-010-9881-2>
- del Arco-Aguilar, M. J., & Rodríguez-Delgado, O. (2018). *Vegetation of the Canary Islands*. Springer. [https://doi.org/10.1007/978-3-319-77255-4\\_7](https://doi.org/10.1007/978-3-319-77255-4_7)
- Dobrowski, S. Z. (2011). A climatic basis for microrefugia: The influence of terrain on climate. *Global Change Biology*, 17(2), 1022–1035. <https://doi.org/10.1111/j.1365-2486.2010.02263.x>
- Dobrowski, S. Z., Abatzoglou, J. T., Greenberg, J. A., & Schladow, S. G. (2009). How much influence does landscape-scale physiography have on air temperature in a mountain environment? *Agricultural and Forest Meteorology*, 149, 1751–1758.
- Dormann, C. F., Elith, J., Bacher, S., Buchmann, C., Carl, G., Carré, G., Marquéz, J. R., Gruber, B., Lafourcade, B., Leitão, P. J., Münkemüller, T., & Lautenbach, S. (2013). Collinearity: A review of methods to deal with it and a simulation study evaluating their performance. *Ecography*, 36(1), 27–46. <https://doi.org/10.1111/j.1600-0587.2012.07348.x>
- Elsen, P. R., Monahan, W. B., & Merenlender, A. M. (2020). Topography and human pressure in mountain ranges alter expected species responses to climate change. *Nature Communications*, 11(1), 1974. <https://doi.org/10.1038/s41467-020-15881-x>
- Elsen, P. R., & Tingley, M. W. (2015). Global mountain topography and the fate of montane species under climate change. *Nature Climate Change*, 5(8), 772–776. <https://doi.org/10.1038/nclimate2656>
- Erickson, K. D., & Smith, A. B. (2023). Modeling the rarest of the rare: A comparison between multi-species distribution models, ensembles of small models, and single-species models at extremely low sample sizes. *Ecography*, e06500. <https://doi.org/10.1111/ecog.06500>
- Finocchiaro, M., Médail, F., Saatkamp, A., Diadema, K., Pavon, D., & Meineri, E. (2023). Bridging the gap between microclimate and microrefugia: A bottom-up approach reveals strong climatic and biological offsets. *Global Change Biology*, 29(4), 1024–1036. <https://doi.org/10.1111/gcb.16526>
- Florencio, M., Patiño, J., Nogué, S., Traveset, A., Borges, P. A. V., Schaefer, H., Amorim, I. R., Arnedo, M., Ávila, S. P., Cardoso, P., de Nascimento, L., & Santos, A. M. C. (2021). Macaronesia as a fruitful arena for ecology, evolution, and conservation biology. *Frontiers in Ecology and Evolution*, 9, 752. <https://doi.org/10.3389/fevo.2021.718169>
- Franklin, J., Davis, F. W., Ikegami, M., Syphard, A. D., Flint, L. E., Flint, A. L., & Hannah, L. (2013). Modeling plant species distributions under future climates: How fine scale do climate projections need to be? *Global Change Biology*, 19(2), 473–483. <https://doi.org/10.1111/gcb.12051>
- Giorgi, F. (2019). Thirty years of regional climate modeling: Where are we and where are we going next? *Journal of Geophysical Research: Atmospheres*, 124(11), 5696–5723. <https://doi.org/10.1029/2018JD030094>
- Giorgi, F., & Lionello, P. (2008). Climate change projections for the Mediterranean region. *Global and Planetary Change*, 63(2), 90–104. <https://doi.org/10.1016/j.gloplacha.2007.09.005>
- Graae, B. J., Vandvik, V., Armbruster, W. S., Eiserhardt, W. L., Svenning, J.-C., Hylander, K., Ehrlén, J., Speed, J. D., Kländerud, K., Bråthen, K. A., Milbau, A., & Lenoir, J. (2018). Stay or go – How topographic complexity influences alpine plant population and community responses to climate change. *Perspectives in Plant Ecology, Evolution and Systematics*, 30, 41–50. <https://doi.org/10.1016/j.ppees.2017.09.008>
- Greiser, C., Ehrlén, J., Meineri, E., & Hylander, K. (2020). Hiding from the climate: Characterizing microrefugia for boreal forest understorey species. *Global Change Biology*, 26(2), 471–483. <https://doi.org/10.1111/gcb.14874>
- Gril, E., Spicher, F., Greiser, C., Ashcroft, M. B., Pincebourde, S., Durrieu, S., Nicolas, M., Richard, B., Decocq, G., Marrec, R., & Lenoir, J. (2023). Slope and equilibrium: A parsimonious and flexible approach to model microclimate. *Methods in Ecology and Evolution*, 14(3), 885–897. <https://doi.org/10.1111/2041-210X.14048>
- Guisan, A., Graham, C. H., Elith, J., Huettmann, F., & NCEAS Species Distribution Modelling Group. (2007). Sensitivity of predictive species distribution models to change in grain size.

- Diversity and Distributions*, 13(3), 332–340. <https://doi.org/10.1111/j.1472-4642.2007.00342.x>
- Guisan, A., Thuiller, W., & Zimmermann, N. E. (2017). *Habitat suitability and distribution models: With applications in R*. Cambridge University Press.
- Haesen, S., Lembrechts, J. J., De Frenne, P., Lenoir, J., Aalto, J., Ashcroft, M. B., Kopecký, M., Luoto, M., Maclean, I., Nijs, I., Niittynen, P., & Van Meerbeek, K. (2021). ForestTemp – Sub-canopy microclimate temperatures of European forests. *Global Change Biology*, 27(23), 6307–6319. <https://doi.org/10.1111/gcb.15892>
- Hall, C. A., & Meyer, W. W. (1976). Optimal error bounds for cubic spline interpolation. *Journal of Approximation Theory*, 16(2), 105–122. [https://doi.org/10.1016/0021-9045\(76\)90040-X](https://doi.org/10.1016/0021-9045(76)90040-X)
- Harter, D. E. V., Irl, S. D. H., Seo, B., Steinbauer, M. J., Gillespie, R., Triantis, K. A., Fernández-Palacios, J. M., & Beierkuhnlein, C. (2015). Impacts of global climate change on the floras of oceanic islands – Projections, implications and current knowledge. *Perspectives in Plant Ecology, Evolution and Systematics*, 17(2), 160–183. <https://doi.org/10.1016/j.ppees.2015.01.003>
- He, X., He, K. S., & Hyvönen, J. (2016). Will bryophytes survive in a warming world? *Perspectives in Plant Ecology, Evolution and Systematics*, 19, 49–60. <https://doi.org/10.1016/j.ppees.2016.02.005>
- Hedenäs, L., Collart, F., Heras, P., Infante, M., Kooijman, A., & Kučera, J. (2022). Distributions and habitats of the two partly allopatric cryptic species of the vulnerable moss *Hamatocaulis vernicosus* (Bryophyta) in Europe. *Botanical Journal of the Linnean Society*, 200(2), 233–254. <https://doi.org/10.1093/botlinnean/boac011>
- Hemer, M. A., Fan, Y., Mori, N., Semedo, A., & Wang, X. L. (2013). Projected changes in wave climate from a multi-model ensemble. *Nature Climate Change*, 3(5), 471–476. <https://doi.org/10.1038/nclimate1791>
- Hijmans, R. J. (2022). *Terra: Spatial data analysis*. R package version 1.6-41. <https://CRAN.R-project.org/package=terra>
- Hodgetts, N. G., Söderström, L., Blockeel, T. L., Caspari, S., Ignatov, M. S., Konstantinova, N. A., Lockhart, N., Papp, B., Schröck, C., Sim-Sim, M., Bell, D., & Porley, R. D. (2020). An annotated checklist of bryophytes of Europe, Macaronesia and Cyprus. *Journal of Bryology*, 42(1), 1–116. <https://doi.org/10.1080/03736687.2019.1694329>
- Hylland, K., Ehrlén, J., Luoto, M., & Meineri, E. (2015). Microrefugia: Not for everyone. *Ambio*, 44(1), 60–68. <https://doi.org/10.1007/s13280-014-0599-3>
- Jerome, H. F. (2001). Greedy function approximation: A gradient boosting machine. *The Annals of Statistics*, 29(5), 1189–1232. <https://doi.org/10.1214/aos/1013203451>
- Jiang, Y., Wang, T., de Bie, C. A. J. M., Skidmore, A. K., Liu, X., Song, S., Zhang, L., Wang, J., & Shao, X. (2014). Satellite-derived vegetation indices contribute significantly to the prediction of epiphyllous liverworts. *Ecological Indicators*, 38, 72–80. <https://doi.org/10.1016/j.ecolind.2013.10.024>
- Jiménez-Valverde, A. (2020). Sample size for the evaluation of presence-absence models. *Ecological Indicators*, 114, 106289. <https://doi.org/10.1016/j.ecolind.2020.106289>
- Karger, D. N., Chauvier, Y., & Zimmermann, N. E. (2023). Chelsa-cmip6 1.0: A python package to create high resolution bioclimatic variables based on CHELSA ver. 2.1 and CMIP6 data. *Ecography*, 2023(6), e06535. <https://doi.org/10.1111/ecog.06535>
- Karger, D. N., Conrad, O., Böhner, J., Kawohl, T., Kreft, H., Soria-Auza, R. W., Zimmermann, N. E., Linder, H. P., & Kessler, M. (2017). Climatologies at high resolution for the earth's land surface areas. *Scientific Data*, 4(1), 170122. <https://doi.org/10.1038/sdata.2017.122>
- Karger, D. N., Nobis, M. P., Normand, S., Graham, C. H., & Zimmermann, N. E. (2021). CHELSA-TraCE21k v1.0. Downscaled transient temperature and precipitation data since the last glacial maximum. *Climate of the Past Discussions*, 2021, 1–27. <https://doi.org/10.5194/cp-2021-30>
- Karger, D. N., Schmatz, D. R., Dettling, G., & Zimmermann, N. E. (2020). High-resolution monthly precipitation and temperature time series from 2006 to 2100. *Scientific Data*, 7(1), 248. <https://doi.org/10.1038/s41597-020-00587-y>
- Knoben, W. J. M., Freer, J. E., & Woods, R. A. (2019). Technical note: Inherent benchmark or not? Comparing Nash–Sutcliffe and Kling–Gupta efficiency scores. *Hydrology and Earth System Sciences*, 23(10), 4323–4331. <https://doi.org/10.5194/hess-23-4323-2019>
- Lange, S. (2019). Trend-preserving bias adjustment and statistical downscaling with ISIMIP3BASD (v1.0). *Geoscientific Model Development*, 12(7), 3055–3070. <https://doi.org/10.5194/gmd-12-3055-2019>
- Lange, S. (2021). *ISIMIP3b bias adjustment fact sheet*. [https://www.isimip.org/documents/413/ISIMIP3b\\_bias\\_adjustment\\_fact\\_sheet\\_Gnsz7CO.pdf](https://www.isimip.org/documents/413/ISIMIP3b_bias_adjustment_fact_sheet_Gnsz7CO.pdf)
- Lee, S., Wolberg, G., & Shin, S. Y. (1997). Scattered data interpolation with multilevel B-splines. *IEEE Transactions on Visualization and Computer Graphics*, 3(3), 228–244. <https://doi.org/10.1109/2945.620490>
- Lembrechts, J. J., & Lenoir, J. (2020). Microclimatic conditions anywhere at any time! *Global Change Biology*, 26(2), 337–339. <https://doi.org/10.1111/gcb.14942>
- Lembrechts, J. J., Lenoir, J., Roth, N., Hattab, T., Milbau, A., Haider, S., Pellissier, L., Pauchard, A., Ratier Backes, A., Dimarco, R. D., Nuñez, M. A., & Nijs, I. (2019). Comparing temperature data sources for use in species distribution models: From in-situ logging to remote sensing. *Global Ecology and Biogeography*, 28(11), 1578–1596. <https://doi.org/10.1111/geb.12974>
- Lembrechts, J. J., Nijs, I., & Lenoir, J. (2019). Incorporating microclimate into species distribution models. *Ecography*, 42(7), 1267–1279. <https://doi.org/10.1111/ecog.03947>
- Lenoir, J., Hattab, T., & Pierre, G. (2017). Climatic microrefugia under anthropogenic climate change: Implications for species redistribution. *Ecography*, 40(2), 253–266. <https://doi.org/10.1111/ecog.02788>
- Leroy, B., Delsol, R., Hugué, B., Meynard, C. N., Barhoumi, C., Barbet-Massin, M., & Bellard, C. (2018). Without quality presence–absence data, discrimination metrics such as TSS can be misleading measures of model performance. *Journal of Biogeography*, 45(9), 1994–2002. <https://doi.org/10.1111/jbi.13402>
- Liu, C., White, M., & Newell, G. (2013). Selecting thresholds for the prediction of species occurrence with presence-only data. *Journal of Biogeography*, 40(4), 778–789. <https://doi.org/10.1111/jbi.12058>
- Lomba, A., Pellissier, L., Randin, C., Vicente, J., Moreira, F., Honrado, J., & Guisan, A. (2010). Overcoming the rare species modelling paradox: A novel hierarchical framework applied to an Iberian endemic plant. *Biological Conservation*, 143(11), 2647–2657. <https://doi.org/10.1016/j.biocon.2010.07.007>
- Maclean, I. M. D. (2020). Predicting future climate at high spatial and temporal resolution. *Global Change Biology*, 26(2), 1003–1011. <https://doi.org/10.1111/gcb.14876>
- Man, M., Wild, J., Macek, M., & Kopecký, M. (2022). Can high-resolution topography and forest canopy structure substitute microclimate measurements? Bryophytes say no. *Science of the Total Environment*, 821, 153377. <https://doi.org/10.1016/j.scitotenv.2022.153377>
- Manzoor, S. A., Griffiths, G., & Lukac, M. (2018). Species distribution model transferability and model grain size – Finer may not always be better. *Scientific Reports*, 8(1), 7168. <https://doi.org/10.1038/s41598-018-25437-1>
- Martín, J. L., Bethencourt, J., & Cuevas-Agulló, E. (2012). Assessment of global warming on the Island of Tenerife, Canary Islands (Spain). Trends in minimum, maximum and mean temperatures since 1944. *Climatic Change*, 114(2), 343–355. <https://doi.org/10.1007/s10584-012-0407-7>
- Marzol, V., Sánchez, J. L., & Yanes, A. (2011). Meteorological patterns and fog water collection in Morocco and the Canary Islands. *Erdkunde*, 65(3), 291–303.
- Mateo, R. G., Broennimann, O., Petitpierre, B., Muñoz, J., van Rooy, J., Laenen, B., Guisan, A., & Vanderpoorten, A. (2015). What is the



- potential of spread in invasive bryophytes? *Ecography*, 38, 480–487. <https://doi.org/10.1111/ecog.01014>
- Meineri, E., Dahlberg, C. J., & Hylander, K. (2015). Using gaussian Bayesian networks to disentangle direct and indirect associations between landscape physiography, environmental variables and species distribution. *Ecological Modelling*, 313, 127–136. <https://doi.org/10.1016/j.ecolmodel.2015.06.028>
- Meineri, E., & Hylander, K. (2017). Fine-grain, large-domain climate models based on climate station and comprehensive topographic information improve microrefugia detection. *Ecography*, 40(8), 1003–1013. <https://doi.org/10.1111/ecog.02494>
- Mittermeier, R. A., Gil, P. R., Hoffmann, M., Pilgrim, J., Brooks, T., Mittermeier, C. G., Lamoreux, J., & Da Fonseca, G. A. (2005). Hotspots revisited: Earth's biologically richest and most endangered terrestrial ecoregions. *Sierra Madre, Cemex*, 315.
- Moore, I. D., Grayson, R. B., & Ladson, A. R. (1991). Digital terrain modelling: A review of hydrological, geomorphological, and biological applications. *Hydrological Processes*, 5(1), 3–30. <https://doi.org/10.1002/hyp.3360050103>
- Moss, R. H., Edmonds, J. A., Hibbard, K. A., Manning, M. R., Rose, S. K., van Vuuren, D. P., Carter, T. R., Emori, S., Kainuma, M., Kram, T., Meehl, G. A., & Wilbanks, T. J. (2010). The next generation of scenarios for climate change research and assessment. *Nature*, 463(7282), 747–756. <https://doi.org/10.1038/nature08823>
- Moudrý, V., Keil, P., Gábor, L., Lecours, V., Zarzo-Arias, A., Barták, V., Malavasi, M., Rocchini, D., Torresani, M., Gdulová, K., Grattarola, F., & Šimová, P. (2023). Scale mismatches between predictor and response variables in species distribution modelling: A review of practices for appropriate grain selection. *Progress in Physical Geography: Earth and Environment*, 47(3), 467–482. <https://doi.org/10.1177/03091333231156362>
- O'Neill, B. C., Tebaldi, C., van Vuuren, D. P., Eyring, V., Friedlingstein, P., Hurtt, G., Knutti, R., Kriegler, E., Lamarque, J. F., Lowe, J., Meehl, G. A., & Sanderson, B. M. (2016). The scenario model Intercomparison project (ScenarioMIP) for CMIP6. *Geoscientific Model Development*, 9(9), 3461–3482. <https://doi.org/10.5194/gmd-9-3461-2016>
- Patiño, J., Bisang, I., Goffinet, B., Hedenäs, L., McDaniel, S., Pressel, S., Stech, M., Ah-Peng, C., Bergamini, A., Caners, R. T., Christine Cargill, D., & Vanderpoorten, A. (2022). Unveiling the nature of a miniature world: A horizon scan of fundamental questions in bryology. *Journal of Bryology*, 44, 1–34. <https://doi.org/10.1080/03736687.2022.2054615>
- Patiño, J., Carine, M. A., Fernández-Palacios, J. M., Otto, R., Schaefer, H., & Vanderpoorten, A. (2014). The anagenetic world of the spore-producing plants. *New Phytologist*, 201, 305–311. <https://doi.org/10.1111/nph.12480>
- Patiño, J., Hedenäs, L., Dirkse, G. M., Ignatov, M. S., Papp, B., Müller, F., González-Mancebo, J. M., & Vanderpoorten, A. (2017). Species delimitation in the recalcitrant moss genus *Rhynchostegiella* (Brachytheciaceae). *Taxon*, 66(2), 293–308. <https://doi.org/10.12705/662.1>
- Patiño, J., Mateo, R. G., Zanatta, F., Marquet, A., Aranda, S. C., Borges, P. A. V., Dirkse, G., Gabriel, R., Gonzalez-Mancebo, J. M., Guisan, A., Muñoz, J., & Vanderpoorten, A. (2016). Climate threat on the Macaronesian endemic bryophyte flora. *Scientific Reports*, 6, 29156. <https://doi.org/10.1038/srep29156>
- Patiño, J., & Vanderpoorten, A. (2018). Bryophyte biogeography. *Critical Reviews in Plant Sciences*, 37(2–3), 175–209. <https://doi.org/10.1080/07352689.2018.1482444>
- Patiño, J., Whittaker, R. J., Borges, P. A. V., Fernández-Palacios, J. M., Ah-Peng, C., Araújo, M. B., Ávila, S. P., Cardoso, P., Cornuault, J., de Boer, E. J., de Nascimento, L., & Emerson, B. C. (2017). A roadmap for Island biology: 50 fundamental questions after 50 years of the theory of Island biogeography. *Journal of Biogeography*, 44(5), 963–983. <https://doi.org/10.1111/jbi.12986>
- Pebesma, E. J., & Bivand, R. S. (2005). Classes and methods for spatial data in R. *R News*, 5, 9–13.
- Pereira, H. M., Leadley, P. W., Proença, V., Alkemade, R., Scharlemann, J. P. W., Fernandez-Manjarrés, J. F., Araújo, M. B., Balvanera, P., Biggs, R., Cheung, W. W., Chini, L., & Walpole, M. (2010). Scenarios for global biodiversity in the 21st century. *Science*, 330, 1496–1501. <https://doi.org/10.1126/science.1196624>
- Potter, K. A., Arthur Woods, H., & Pincebourde, S. (2013). Microclimatic challenges in global change biology. *Global Change Biology*, 19(10), 2932–2939. <https://doi.org/10.1111/gcb.12257>
- Press, W. H., Flannery, B. P., Teukolsky, S. A., & Vetterling, W. T. (1989). *Numerical recipes*. Cambridge University Press.
- Proctor, M. C. F., Oliver, M. J., Wood, A. J., Alpert, P., Stark, L. R., Cleavitt, N. L., & Mishler, B. D. (2007). Desiccation-tolerance in bryophytes: A review. *The Bryologist*, 110(4), 595–621.
- Randin, C. F., Engler, R., Normand, S., Zappa, M., Zimmermann, N. E., Pearman, P. B., Vittzo, P., Thuiller, W., & Guisan, A. (2009). Climate change and plant distribution: Local models predict high-elevation persistence. *Global Change Biology*, 15(6), 1557–1569. <https://doi.org/10.1111/j.1365-2486.2008.01766.x>
- Rull, V. (2009). Microrefugia. *Journal of Biogeography*, 36(3), 481–484. <https://doi.org/10.1111/j.1365-2699.2008.02023.x>
- Rummukainen, M. (2010). State-of-the-art with regional climate models. *WIREs Climate Change*, 1(1), 82–96. <https://doi.org/10.1002/wcc.8>
- Santini, L., Benítez-López, A., Maiorano, L., Čengić, M., & Huijbregts, M. A. J. (2021). Assessing the reliability of species distribution projections in climate change research. *Diversity and Distributions*, 27(6), 1035–1050. <https://doi.org/10.1111/ddi.13252>
- Santos, F. D., Valente, M. A., Miranda, P. M. A., Aguiar, A., Azevedo, E. B., Tomé, A. R., & Coelho, F. (2004). Climate change scenarios in the Azores and Madeira islands. *World Resource Review*, 16(4), 473–491.
- Scherrer, D., & Körner, C. (2010). Infra-red thermometry of alpine landscapes challenges climatic warming projections. *Global Change Biology*, 16(9), 2602–2613. <https://doi.org/10.1111/j.1365-2486.2009.02122.x>
- Seo, C., Thorne, J. H., Hannah, L., & Thuiller, W. (2008). Scale effects in species distribution models: Implications for conservation planning under climate change. *Biology Letters*, 5(1), 39–43. <https://doi.org/10.1098/rsbl.2008.0476>
- Shen, T., Corlett, R. T., Collart, F., Kasprzyk, T., Guo, X.-L., Patiño, J., Su, Y., Hardy, O. J., Ma, W.-Z., Wang, J., Wei, Y.-M., Mouton, L., Li, Y., Song, L., & Vanderpoorten, A. (2022). Microclimatic variation in tropical canopies: A glimpse into the processes of community assembly in epiphytic bryophyte communities. *Journal of Ecology*, 110, 3023–3038. <https://doi.org/10.1111/1365-2745.14011>
- Smith, A. B., Godsoe, W., Rodríguez-Sánchez, F., Wang, H.-H., & Warren, D. (2019). Niche estimation above and below the species level. *Trends in Ecology & Evolution*, 34(3), 260–273. <https://doi.org/10.1016/j.tree.2018.10.012>
- Stark, J. R., & Fridley, J. D. (2022). Microclimate-based species distribution models in complex forested terrain indicate widespread cryptic refugia under climate change. *Global Ecology and Biogeography*, 31(3), 562–575. <https://doi.org/10.1111/geb.13447>
- Suggitt, A. J., Wilson, R. J., Isaac, N. J. B., Beale, C. M., Auffret, A. G., August, T., Bennie, J. J., Crick, H. Q., Duffield, S., Fox, R., Hopkins, J. J., & Maclean, I. M. D. (2018). Extinction risk from climate change is reduced by microclimatic buffering. *Nature Climate Change*, 8(8), 713–717. <https://doi.org/10.1038/s41558-018-0231-9>
- Syfert, M. M., Smith, M. J., & Coomes, D. A. (2013). The effects of sampling bias and model complexity on the predictive performance of MaxEnt species distribution models. *PLoS One*, 8(2), e51518.

- Tapiador, F. J., Navarro, A., Moreno, R., Sánchez, J. L., & García-Ortega, E. (2020). Regional climate models: 30 years of dynamical downscaling. *Atmospheric Research*, 235, 104785. <https://doi.org/10.1016/j.atmosres.2019.104785>
- Thuiller, W., Georges, D., Gueguen, M., Engler, R., Breiner, F., Lafourcade, B., & Patin, R. (2022). *biomod2: Ensemble platform for species distribution modeling*. R package version 4.2-1.
- Thuiller, W., Guéguen, M., Renaud, J., Karger, D. N., & Zimmermann, N. E. (2019). Uncertainty in ensembles of global biodiversity scenarios. *Nature Communications*, 10(1), 1446. <https://doi.org/10.1038/s41467-019-09519-w>
- Tokarska, K. B., Stolpe, M. B., Sippel, S., Fischer, E. M., Smith, C. J., Lehner, F., & Knutti, R. (2020). Past warming trend constrains future warming in CMIP6 models. *Science Advances*, 6(12), eaaz9549. <https://doi.org/10.1126/sciadv.aaz9549>
- Tuba, Z., Slack, N. G., & Stark, L. R. (2011). *Bryophyte ecology and climate change*. Cambridge University Press.
- Vanderpoorten, A., Laenen, B., Rumsey, F., González-Mancebo, J., Gabriel, R., & Carine, M. (2011). Dispersal, diversity and evolution of the Macaronesian cryptogamic floras. In D. Bramwell & J. Caujapé-Castells (Eds.), *The biology of Island floras* (pp. 383–364). Cambridge University Press.
- Varela, S., Anderson, R. P., García-Valdés, R., & Fernández-González, F. (2014). Environmental filters reduce the effects of sampling bias and improve predictions of ecological niche models. *Ecography*, 37(11), 1084–1091. <https://doi.org/10.1111/j.1600-0587.2013.00441.x>
- Whittaker, R. J., & Fernández-Palacios, J. M. (2007). *Island biogeography: Ecology, evolution and conservation* (2nd ed.). Oxford University Press.
- Zanatta, F., Engler, R., Collart, F., Broennimann, O., Mateo, R. G., Papp, B., Muñoz, J., Baurain, D., Guisan, A., & Vanderpoorten, A. (2020). Bryophytes are predicted to lag behind future climate change despite their high dispersal capacities. *Nature Communications*, 11(1), 5601. <https://doi.org/10.1038/s41467-020-19410-8>
- Zevenbergen, L. W., & Thorne, C. R. (1987). Quantitative analysis of land surface topography. *Earth Surface Processes and Landforms*, 12(1), 47–56. <https://doi.org/10.1002/esp.3290120107>
- Zurell, D., Franklin, J., König, C., Bouchet, P. J., Dormann, C. F., Elith, J., Fandos, G., Feng, X., Guillera-Arroita, G., Guisan, A., Lahoz-Monfort, J. J., & Merow, C. (2020). A standard protocol for reporting species distribution models. *Ecography*, 43(9), 1261–1277. <https://doi.org/10.1111/ecog.04960>

## BIOSKETCHES

**Jairo Patiño** is a researcher at Instituto de Productos Naturales y Agrobiología (IPNA-CSIC) interested in island biogeography and the study of ecological and evolutionary processes shaping changes in the distribution of biodiversity facets over time and space. Additional information about the laboratory and ongoing research projects can be found at <http://iecoevolab.com/>.

**Flavien Collart** is a postdoctoral researcher interested in the biogeography of land plants, mainly bryophytes. His research focusses on species distributions across space and time by characterizing species ecological niches.

Author contributions: JP, DNK, AV, and FC conceived and designed this study, wrote the first draft of the manuscript, with significant contributions from the rest of authors. JP and AV compiled the species occurrences. JLME and AN-C provided the climate station data. DNK, FC, and SM performed the downscaling analyses. JP and FC analysed the data.

## SUPPORTING INFORMATION

Additional supporting information can be found online in the Supporting Information section at the end of this article.

**How to cite this article:** Patiño, J., Collart, F., Vanderpoorten, A., Martin-Esquivel, J. L., Naranjo-Cigala, A., Mirolo, S., & Karger, D. N. (2023). Spatial resolution impacts projected plant responses to climate change on topographically complex islands. *Diversity and Distributions*, 00, 1–18. <https://doi.org/10.1111/ddi.13757>